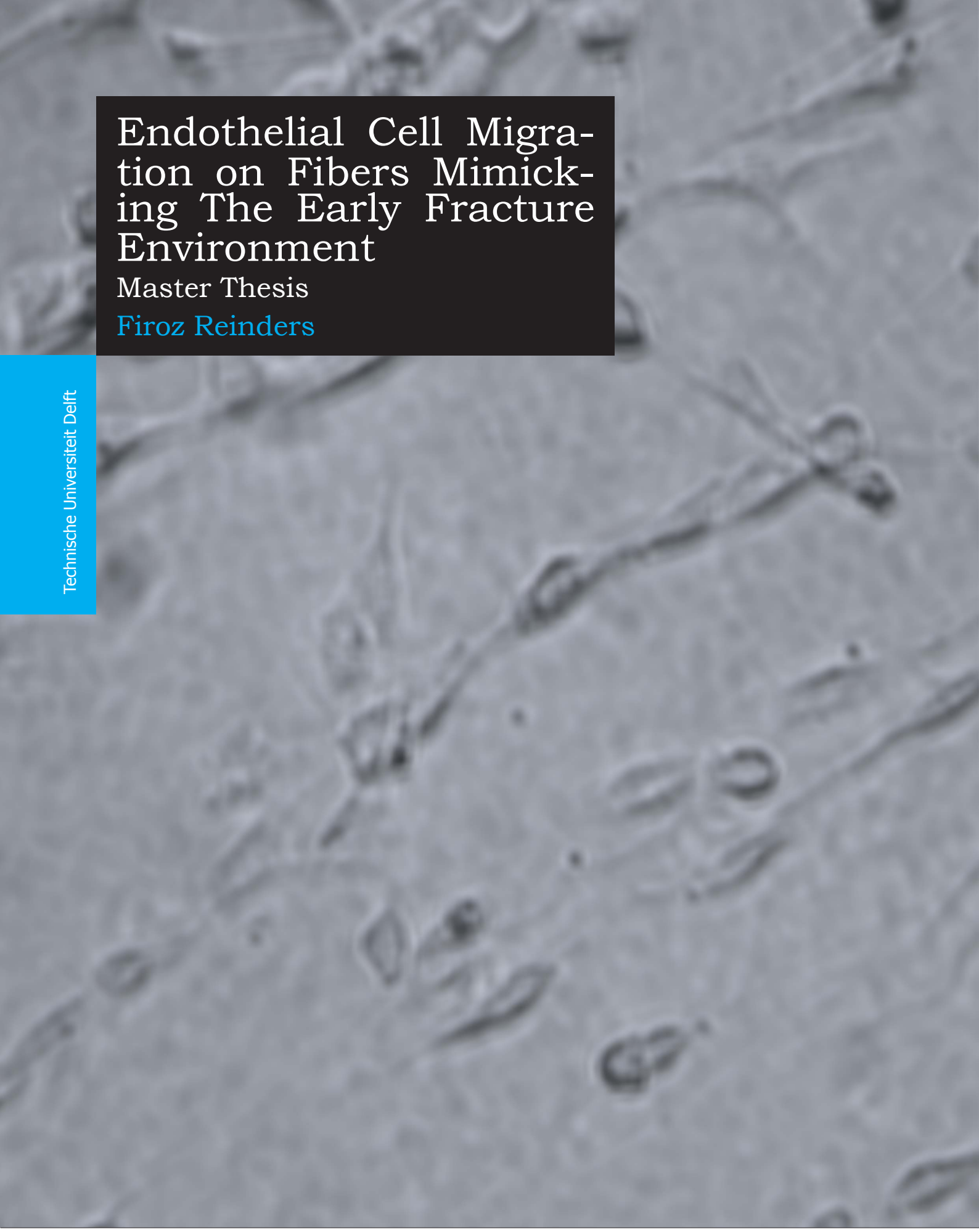

Endothelial Cell Migration on Fibers Mimicking The Early Fracture Environment

Master Thesis

Firoz Reinders

Technische Universiteit Delft

TU Delft Delft University of Technology

Challenge the future

Endothelial Cell Migration on Fibers Mimicking The Early Fracture Environment

Master Thesis

by

Firoz Reinders

in partial fulfillment of the requirements for the degree of

Master of Science
in Biomedical Engineering

Student number: 4599314
Submission Date: 06/07/2018
Supervisor: Dr. ir. L. Fratila-Apachitei, TU Delft
Dr. Y. Y. S. Huang, University of Cambridge
Prof. dr. A. Zadpoor, TU Delft

TU Delft Delft University of Technology

Abstract

Bone is a tissue with many important functions, such as structural support, organ protection and mineral homeostasis. Additionally, after trauma, it can naturally regenerate into fresh, fully functional bone tissue. However, several factors can significantly impede the healing process and cause the formation of non-union tissue. Costs for hospitalization and treatments that prevent such non-unions can become a significant personal and socio-economic burden. To develop more efficient treatments that can tackle this, a thorough understanding of the bone fracture healing process is needed. It is currently known that bone heals via a multistage sequential process of inflammation, soft-callus formation, hard-callus formation and then bone remodelling. Moreover, during this process there is a need for restoration of a vascular network for nutrient delivery and waste removal. Whereas the regulation of vascular network during later stages is understood, knowledge of the mechanisms and driving forces of vascularization during earlier phases in bone healing is currently lacking. Nevertheless, during this process, cell migration towards the site of fracture is of great importance. This process is affected through a range of extracellular signals, which are dependent on the properties of the extracellular matrix. It has been shown that the structural properties and the composition of the fracture tissue are two of the key regulators in guiding cellular migration. This study has integrated the use of a novel electrospinning technique to mimic the effects of the early fracture composition on (endothelial) cell migration. Fibrinogen and gelatin fibers, which are reflective of the early fracture environment, have been spun using an acidic solvent system. Characterization of the fibers showed that the electrospinning process caused minor changes in the protein structure of fibrinogen, and none in that of gelatin. Furthermore, endothelial cells were cultured with a cell free zone on top of fibrinogen and gelatin patterned substrates to mimic cell migration during fracture revascularization. Cellular migration increased with higher fiber density, and gelatin fibers generally showed higher rates of cell migration. Furthermore, gelatin fibers showed higher amounts of cell polarization than fibrinogen fibers, likely driven by the higher stiffness of gelatin fibers. Moreover, the addition of fibers showed to reflect different modes of in vivo vascularization of cell migration on the substrates. To further analyze the effects of fracture composition on endothelial cell migration, fiber membranes were electrospun on a transwell-like device, and cell migration from a fibrin gel was assessed. The physical constraints posed by the fiber membranes were shown to impede cellular migration from the fibrin gel, and no significant differences were found between cell migration on the membranes. Overall, it became evident that the structural properties and the composition of the fibrous micro-environment regulate cellular migration, and can in turn affect the bone regeneration as a whole. Ultimately, further optimization and characterization of the used models are needed, such that they can more closely reflect the fracture healing environment.

Abbreviations and Acronyms

DI Water	Deionized Water
ECM	Extracellular Matrix
FBS	Fetal Bovine Serum
FTIR(S)	Fourier Transform Infrared (Spectroscopy)
LEP	Low Voltage Electrospinning Patterning
PBS	Phosphate Buffered Saline
UV	Ultra Violet
VEGF	Vascular Endothelial Growth Factor

Contents

List of Figures

List of Tables

1

Introduction

1.1. Bone Healing

Bone fulfills a plethora of crucial functions in the body, such as structural support and organ protection. It also acts as an attachment site for muscles to allow for locomotion, and acts as a mineral reservoir for electrolytes [7]. As such, bone fractures can show to be a significant burden on individuals. Studies have shown that 3.6% of the UK population (about 2.4 million people) are estimated to suffer from bone fractures yearly [8]. Whereas bones have the ability to self-heal, some fractures do not heal properly and instead form a non-union. Such non unions contain excessive amounts of soft tissue instead of bone tissue, and fail to fulfill the multiple roles of bone [9]. Currently, about 10% of all bone fractures is estimated to lead to the formation of non-union [10]. As such, non-unions and the prevention thereof additionally cause bone fractures to be a large socio-economic problem. For example, hospitalization costs of hip fracture patients alone were £1.1 billion in 2016 [11]. Additionally, bone fractures and non-unions will grow increasingly common with an aging population, increased numbers of obesity and poor physical activity [10]. A thorough understanding the natural process of bone fracture healing will allow the development of new treatments and materials that can prevent the formation of non-unions.

In vivo, natural bone fracture healing occurs through a set of four interrelated but distinguished phases: inflammation, soft callus formation, hard callus formation and bone remodeling [12]. These phases are schematically depicted in Figure 1.1. Directly after trauma during the inflammatory phase, a fibrin hematoma forms that entraps a range of important cytokines and growth factors that aid the recruitment of inflammatory cells. These inflammatory cells clean debris from the fracture site, and cause the recruitment of new mesenchymal stem cells (MSCs). In turn, these MSCs differentiate into cells with fibrogenic potential (i.e. fibroblasts, and deposit fresh collagen to form a soft granular callus. The formation of fresh vasculature is initiated during the soft callus phase of fracture healing, and is further regulated during the hard callus phase and bone remodeling. Revascularization of the fracture tissue is of key importance for succesful bone regeneration. Blood vessels are needed for the supply of nutrients and cells, and removal of waste [12]. During vascularization, endothelial cells form new capillaries *in situ* (vasculogenesis), or grow out into the fracture tissue from existing vessels (angiogenesis) [13]. Regulation of vessel growth in later stages of the fracture callus is known to be driven by complex signalling processes involving vascular growth factors (i.e. VEGF) and endothelial cells, but the mechanisms driving vessel formation during earlier phases remains largely unknown [14]. In the hard callus phase, MSC derived chondrocytes initiate the calcification of the collagenous matrix to form a hard callus that resembles fresh bone. Finally, bone is remodeled by bone cells in response to mechanical loads until it is indistinguishable from healthy bone. Briefly, osteocytes sense mechanical signals and in turn either stimulate osteoclasts (bone resorbing cells) or osteoblasts (bone depositing cells) to resorb bone at low and high mechanical loads respectively.

To properly understand the processes involved in bone fracture healing, it is essential to review the role of the biological, chemical, physical and mechanical factors involved.

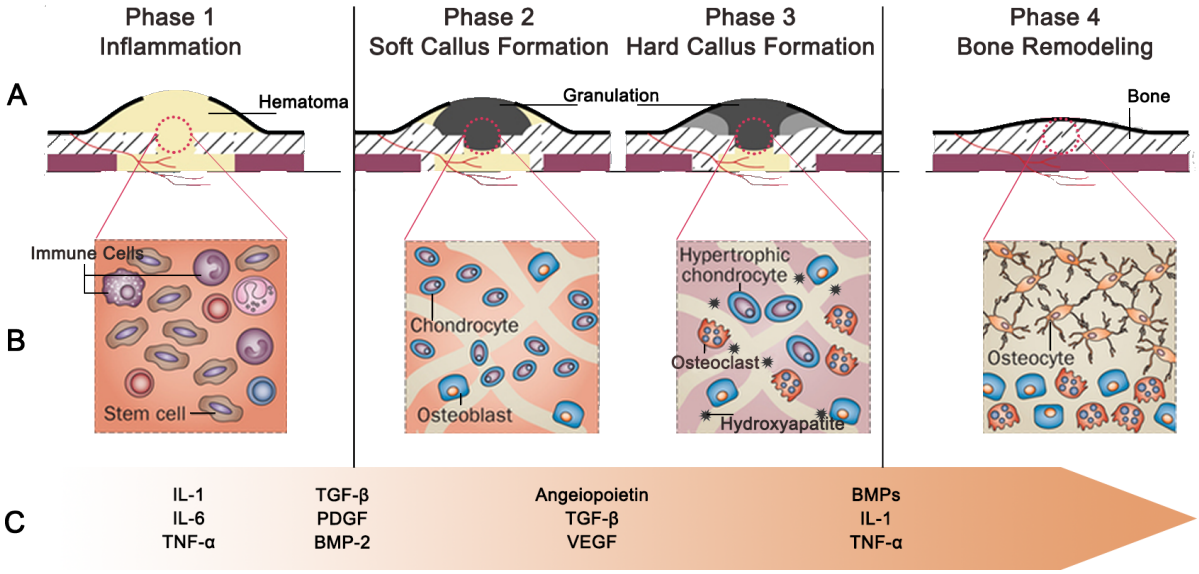

Figure 1.1: [A] The phases of fracture healing: Inflammation, soft callus formation, hard callus formation, and bone remodeling. Adapted from [1]. [B] The main cells involved during each fracture healing phase. Adapted from [2]. [C] The main signalling molecules involved during the fracture regeneration process. Adapted from [3, 4].

1.1.1. Key Players in Fracture Healing

A common model in bone tissue engineering that places these factors in the framework of fracture healing is given by Giannoudis et al. [15]: the diamond concept of fracture healing. Following this concept, successful fracture healing is determined by the involved cellular components, scaffold properties, cytokines and growth factors, and mechanical loads, and the crosstalk between them. Consequently, when the balance in these different elements is disturbed during any of the phases of bone regeneration, it can delay or prevent the formation of a proper union of the fracture ends.

The in vivo regeneration process is the result of the activities of multiple cell types [12, 16]. Some of the important cellular components of this regenerative process are outlined in Figure 1.1.B. To illustrate, early on, immune cells are responsible for cleaning necrotic tissue at the fracture site. Later, endothelial cells are needed for the formation of new vasculature. A range of cells that regulate neotissue formation are derived from mesenchymal cells, such as fibroblasts and chondrocytes during soft-callus formation, and osteoblasts, osteoclasts and osteocytes during hard callus-formation and bone remodeling [12, 16]. Furthermore, the properties of the involved scaffolds directly influence bone healing. For example, surface nano- and microtopography can directly regulate cell differentiation and activity [17, 18]. Moreover, properties such as pore size and pore connectivity directly influence ingrowth of new tissue by regulating cell infiltration [19, 20]. For instance, dense fibrous hematomas consisting of thin fibers have been associated with decreased bone formation as opposed to porous hematomas with thick fibers [21]. Cytokines and growth factors influence cell behaviour and ultimately tissue properties. They cause the timely migration of the proper cell types and induce MSC differentiation and in this way regulate the type of tissue formed. For example, a prolonged expression of inflammatory cytokines can cause the formation of excessive soft tissue and impede the formation of healthy bone [22, 23]. Lastly, mechanical cues directly influence the type of tissue formed at the fracture site [15]. Whereas the early fracture tissue does not allow for much loading due to its low stiffness, the fracture tissue is sequentially remodeled into stiffer tissue that progressively allows for higher loads. Some studies show that early callus stiffness can serve as a strong predictor of bone regeneration as it influences the tissue strain during loading [24, 25]. Later on, during the remodeling phase, mechanical loads cause fluid flow in the interstitial spaces of the extracellular matrix. Bone lining cells and osteocytes experience the shear stress caused by these flows. They then stimulate bone deposition in response to higher loads, and vice versa [26]. As such, these biological, chemical, physical and mechanical factors all influence fracture healing via a complex interplay.

1.2. Cell Migration and the Role of the Fracture Microenvironment

As described previously, a supply of fresh cells is constantly needed to aid in the fracture healing process. Early on, there is a need for inflammatory cells, whereas later on mesenchymal stem cells are needed to differentiate and remodel the fracture site. Additionally, endothelial cells invade the fracture to form a new vascular system. Lastly, during bone remodeling, a multitude of different bone cells constantly move around the fracture to remodel the hard callus in response to mechanical loads.

Cellular migration is the directed movement of cell, and several distinct steps can be distinguished [5]. Firstly, the cytoskeletal structure of the cell is reorganized in response to some extracellular cue (Figure 1.2.i). The cell becomes polarized and forms protrusions in the direction of migration (Figure 1.2.ii). Then, These protrusions reattach to the ECM or other cells [27] (Figure 1.2.iii). The binding of the cells to the micro-environment then allows the cells to exert traction forces (Figure 1.2.iv). As such, when releasing attachment to the micro-environment at the rear of the cell (Figure 1.2.v), a net displacement can be found before the process is repeated (Figure 1.2.vi).

The described process paints an image of single cell migration through a cyclic sequence of polarization and contraction. During fracture healing, many cells individually migrate constantly, such as during immune cell migration in the inflammatory phase, and endothelial cell migration during vasculogenesis [5, 12]. However, many cells move and infiltrate the ECM without the disruption of cell-cell junctions, for example during angiogenesis [13, 28]. Such collective cell migration shows many similarities to single cell migration, but also involves the collective polarization of a large group of cells without disrupting intercellular junctions [29]. There are three main categories that drive cell migration that can be distinguished [5], with much resemblance to the key players during fracture healing: chemotaxis, haptotaxis and mechanotaxis. Chemotaxis describes the tendency of cells to migrate in response to a chemical gradient found in the micro-environment. For example, during fracture healing, the type of cell that migrates is regulated via a range of cytokines and growth factors. For example, during the soft-callus phase, endothelial cells are recruited to form new vasculature by vessel-stimulating growth factors [28]. Furthermore, during haptotaxis, the properties of the ECM play an important role. For example, the number of available sites that allow cell integrins to attach to the ECM can directly influence migration [27, 30]. Furthermore, mechanical properties such as stiffness can directly influence migration. It is known that stiffer substrates allow cells to exert higher contractile forces and in this way increase migratory potential [31, 32]. Lastly, mechanotaxis regulates cell behaviour and migration directly via mechanical cues. For example, shear stress directly influences endothelial cell migration by altering cell shape and increasing cell polarization [33].

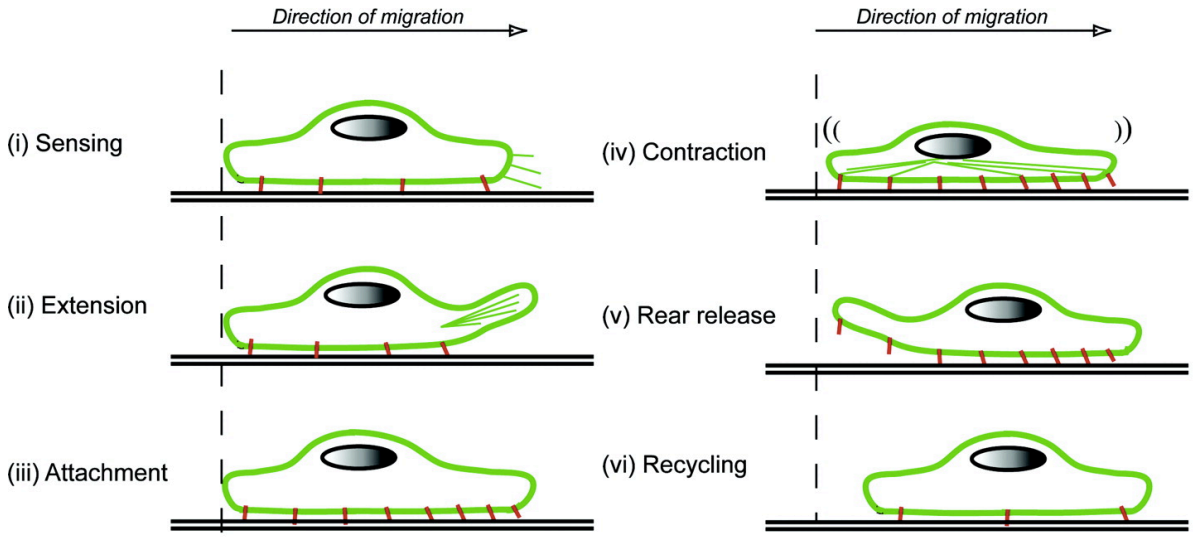

Figure 1.2: The main steps during cell migration. (i) The cell is stimulated via extracellular signals to start migrating. (ii) It starts forming extensions towards the direction migration and (iii) reattaches to the ECM. (iv) By contraction and (v) release of the rear side, there is a net displacement (vi) of the cell. Image adapted from [5].

As such, it is known that the micro-environment can directly influence cellular migration. On the

other hand, the exact mechanisms through which these extracellular cues drive cell behaviour are still largely unknown [34]. Furthermore, these different signals are in constant competition for driving cell behaviour, and their interplay is currently not well understood. A thorough understanding of the factors that drive cells to migrate into the fracture site is promising for developing effective treatments and artificial tissues that aid bone regeneration.

1.3. Electrospinning for Tissue Mimicry

It has been shown to be technologically challenging to investigate direct cell behaviour and ECM interactions in vivo [35]. As such, significant advancements have been made in engineering systems that allow for studying cell behaviour in bone and fracture like tissues in vitro [36]. One technique that allows mimicry of the fibrous properties of the early fracture hematoma is the electrospinning process. In the electrospinning process, an electrified jet of polymer solution is created using the application of a high voltage to draw microfibers onto a grounded substrate. In conventional electrospinning processes, it is possible to significantly increase electrostatic repulsion forces within the polymer solution by electrically charging the solution, using high voltages in the range of tens of kilovolts. The electrostatic repulsion causes the formation of a conical droplet at the nozzle called a Taylor cone. When the voltage is significantly large, the electrostatic repulsion overcomes the surface tension of the droplet and an unstable, whipping polymer jet is formed between the charged tip and collector. During travel, the electrified jet elongates continuously, causing the formation of a thin jet that travels towards the collector. Furthermore, as the jet is stretches, solvent evaporates, and polymer fibers down to tens of nanometers can be formed [37]. Traditional electrospinning processes operate at high voltages and relatively large distances (tens of centimeters), causing the formation of a whipping jet at the end of the jet travel path, causing the formation of randomly oriented fibers. As such, controllable deposition of fibers on versatile substrates can pose to be a significant hassle. Recently, a low voltage continuous electrospinning patterning (LEP) technique has been developed [6] which allows for the controlled template free deposition of micro- and nanofibers using voltages in the range of hundreds of volts. Instead of high voltages, the LEP process uses mechanical initiation of the polymeric jet, which is subsequently sustained by a low voltage, as shown in Figure 1.3.

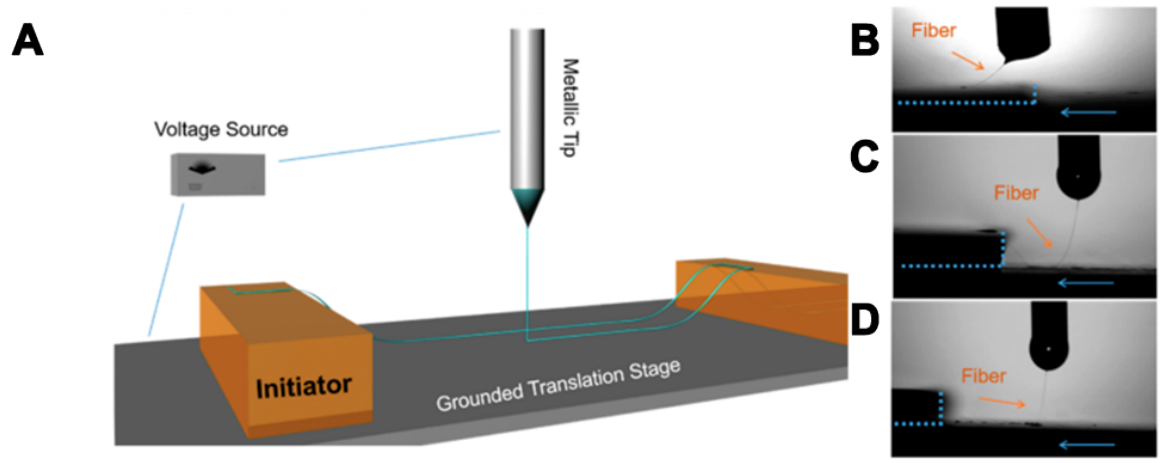

Figure 1.3: [A] Overview of the low voltage electrospinning process. A metallic tip from which a solution is ejected is positively charged. [B, C, D] Fibers are initiated using a mechanical drawing process and sustained using an electric field. Image adapted from [6]

Electrospinning has been previously used to fabricate gelatin fibers [38], a natural polymer that closely resembles the collagenous tissue found in the soft callus. Furthermore, fibrinogen fiber scaffolds can be electrospun to contain properties reflective of the fibrin hematoma that is found during the inflammatory phase [39]. Furthermore, it has been shown that the use of electrospun fiber patterns on substrates can be used to properly resemble the migration behaviour of cells as in the in vivo micro-environment [40, 41].

1.4. Objective of the Research

It has been established that a thorough understanding of the processes involved in fracture healing is needed to develop novel treatments. In this study, we establish the use of this LEP technique to create fibrinogen and gelatin fiber patterned substrates as an early fracture ECM mimic for studying cellular migration in vitro. First, gelatin and gelatin-fibrinogen blend fibers were developed using existing protocols, and a new protocol for electrospinning fibrinogen has been developed. Second, the nanofibers have been integrated in different wound healing assays via adaptation of existing models by using additively manufactured devices. Cell migration along fibers is assessed using fibers spun on flat surfaces, and observing the cellular migration onto a cell free zone [42] (Figure 1.4.B). Lastly, to asses cell migration through a fibrous matrix, a transwell inspired device has been developed [42] (Figure 1.4.C). As such, we will look at the development of cell migration assays integrating fiber compositions that reflect the early fracture tissue.

Therefore, the research goal of this thesis can be summarized as follows:

- Development of electrospun fibrinogen and gelatin fibers that reflect the early bone environment.
- Incorporation of these fibers into various cellular migration models to study assess the effect of early fracture microenvironment.

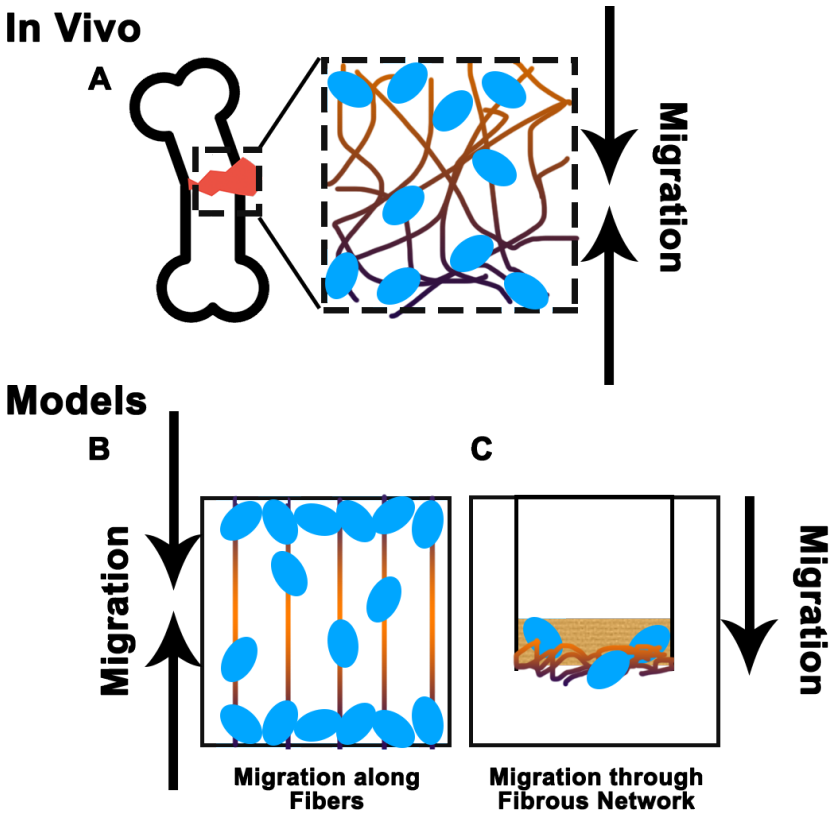

Figure 1.4: [A] Schematic depiction of cell migration during bone fracture in vivo. [B] Model of cell migration in which cells can migrate along fibers on a substrate, similarly as they would in vivo. [C] Model of cell migration through a network of fibers.

This study uses Ea.Hy926, an endothelial cell line, and thus reflects vascularization during the early regeneration phases. It has been shown that migration of endothelial cells is done via similar processes as cell migration of many different types of cells involved in fracture healing [5, 42], and can as such also show a more general insight in the effect of fibers and fiber composition on cell migration. Nevertheless, the models are designed to allow for culture and assessment of different cell types that can reflect different aspects in the fracture regeneration process.

2

Materials and Methods

All chemicals described are obtained from Sigma-Aldrich, unless indicated differently.

2.1. Fiber Spinning

The basic setup for electrospinning is depicted in Figure 2.1. It consisted of two computer controlled linear motor stages (Thorlabs, DDSM100) that were orthogonally bolted together using an adapter plate (Thorlabs, DDSMP1XY). A syringe pump (World Precision Instruments, AL-1000) was loaded with a plastic syringe (BD Plastipak) containing 1 mL of electrospinning solution. The syringe was connected to a metallic needle (BD Microlance, 19G) with a blunt tip. The syringe needle was connected to a positive voltage supply. A metallic collector plate was attached to the ground of the voltage supply. A vertically adjustable Z-stage (Thorlabs, L490MZ/M) was used to tune the height between the needle and collector, and was set 1 mm above the grounded substrate. A small droplet (1 μL) was ejected, and glass slides were used as mechanical initiators to aid in the electrospinning process. A fume extraction head was placed to cover the setup during electrospinning. Modifications of the electrospinning setup were performed where needed to aid the spinning on printed substrates.

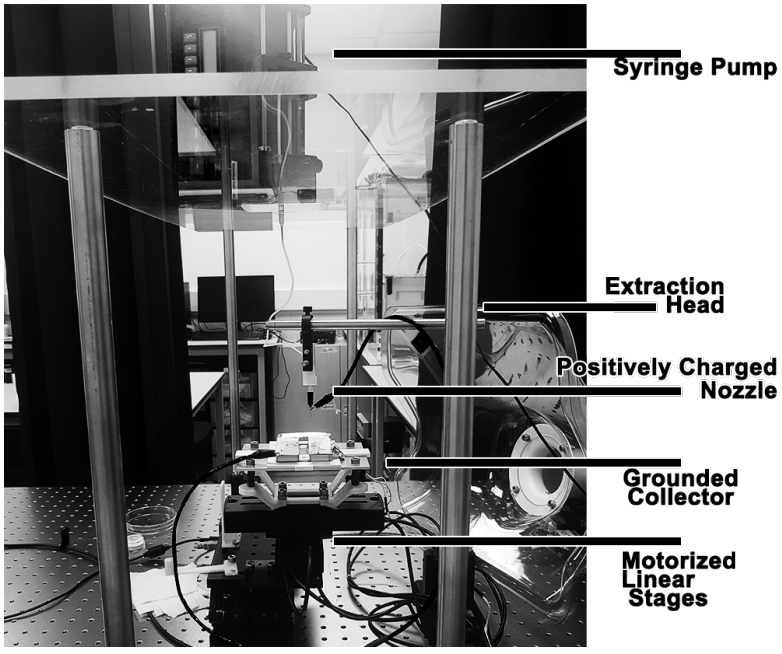

Figure 2.1: Setup for electrospinning fibers. The syringe pump is connected to a metallic nozzle. This nozzle is positively charged by a voltage supply (not shown). On top of the grounded collector a set of glass slides is used to initiate the fiber drawing process. The collector stage is grounded and set on top of two independently movable motorized linear stages.

2.1.1. Electrospinning of Gelatin

Gelatin solution was electrospun using previously described protocols [43]. Shortly, a 19wt% gelatin solution was prepared by dissolving 1mg gelatin (porcine gelatin powder, gel strength 300, Type A) in a solution of acetic acid (Fisher Scientific), ethyl acetate and DI water at a ratio of 19:26:33:22. The gelatin is solved overnight with the aid of a magnetic stirrer. Then, 1 mL of solution was taken with a syringe and loaded in the electrospinning setup, after which fibers were spun using the described protocol. Setup parameters were determined experimentally. To crosslink fibers, a droplet of 20μL of 40wt% glyoxial is added to the spun fibers and allowed to cover the fibers. Fibers were directly washed with PBS to remove excess crosslinker. Before cell culture, fibers are washed again overnight using PBS.

2.1.2. Electrospinning Fibrinogen

To find an appropriate solvent system that allows for electrospinning fibrinogen, its solubility was tested using a range of common solvents: Phosphate Buffered Saline (PBS) (GIBCO/Thermo Scientific), DI Water, ethanol and acetic acid. Shortly, different amounts (60mg, 120mg, 160mg) of frozen fibrinogen powder (bovine fibrinogen powder, Type I-S, 65-85% protein) were weighed out and added to a glass vial. Subsequently, 1 mL of solvent was pipetted on to the fibrinogen powder, and left to dissolve overnight at 37 °C. The solution was observed by eye after 24 hours for leftover protein, and rated for solubility.

Afterwards, a blend of good solvents was tested for electrospinning. To test the electrospinnability of a solution, 1mL of the solution was loaded in a plastic syringe and spun as described previously. Appropriate electrospinning parameters were determined experimentally. Successful electrospinning was achieved using a solution 100 mg/ml Fibrinogen solved in PBS and acetic acid in a 3:1 ratio. All further experiments were done using fibers spun at 100V with a flow rate of 12μL/hr. Fibers were similarly prepared with crosslinker as gelatin fibers using 40wt% glyoxal. Before cell culture, fibers were washed again overnight using PBS.

2.1.3. Chemical Characterisation of Fibers

The use of an acidic solvent system can cause changes in the protein structure. As such, chemical characterisation of electrospun fibers is done using Fourier Transform Infrared (FTIR) spectroscopy (JASCO, Spectron 4000). The spectrum used ranged from a wavelength of 400cm^{-1} to 4000cm^{-1} with a resolution of 4cm^{-1}. Electrospun fibers were fabricated following protocol, and then pulverized using tweezers to form a fine powder. Additionally, unprocessed gelatin and fibrinogen powders are analyzed as a comparison. Absorbance spectra are normalized and their baseline is shifted to allow for comparison.

2.2. Cell Culturing

2.2.1. Sample preparation

To prepare substrates containing electrospun fibers, glass slides (18mm x 18mm) were prepared by washing in ethanol and drying before electrospinning. Then, fiber drawing of gelatin and fibrinogen was performed using the described protocol. The distance between fibers was adjusted via the programming of the linear stage and set to 60μm and 120 μm to create substrates with different fiber densities. Substrates were tested containing 60 μm spacing between fibrinogen (FIB60) or gelatin fibers (GEL60), and 120 μm spacing between fibrinogen (FIB120) or gelatin (GEL120) fibers. Glass slides with no fibers were used as a control. Samples were prepared for cell seeding by 20 minutes exposure to UV, and submersion in PBS overnight at 37°C.

2.2.2. Cell Pre-Culturing

EA.hy926 cells were maintained in a T-25 flask in Dulbecco's Modified Eagle Medium (GIBCO/Thermo Scientific) that was supplemented with 10v% Fetal Bovine Serum (FBS) (GIBCO/Thermo Scientific) and 1v% penicilin-streptomycin (GIBCO/Thermo Scientific). Flasks were incubated in 5% CO_2 at 37°C, and medium was refreshed every other day. Before cell seeding on any substrates, cells were washed with 5mL PBS, trypsinized to deattach, and centrifuged at 1000 RPM for 5 minutes to form a cell-pellet. Cells were then resuspended in medium and counted using a hemacytometer and trypan blue staining to exclude dead cells and debris. Cell concentration was diluted as needed.

2.2.3. Cell Viability Assay

Cell viability was tested by seeding 3 mL of cells in a 6-well containing glass slides with fibers (either 60 μm fiber spacing or 120 μm fiber spacing) at a seeding density of $0.2x10^6$ cells/mL. Cells were counted after 24 hours and 48 hours after trypsinization using a hemacytometer and trypan blue staining to count viable cells. Before trypsinization, cell medium was refreshed to remove unattached cells. Then, number of cells per growth area (cells/mm^{-2}) is calculated. Additionally, viability of cells on electrospun samples (V_{es}) was given as a fraction of viable cells on the control sample (V_{contr}):

$$Viability = \frac{V_{es}}{V_{contr}} \tag{2.1}$$

2.2.4. Cell Free Zone Migration Assay

To measure collective migration of cells, a cell free zone migration assay is used [42]. This migration assay was performed using a additively manufactured cell exclusion device. Briefly, a bounding box was designed (Onshape Inc., Onshape) (see Figure 2.2.A) that allows to split cell culture area in two with a cell free zone. Then, a fused filament printer (Ultimaker B.V., Ultimaker 3) was used to print the designs using ABS. Printing was done using a layer height of 100 μm and an infill density of 100%. After printing, the structure slightly sanded down to the appropriate dimensions. Then, the excluder was immersed in water until use to avoid floating during placement in culture. Shortly before use in cell culture, devices were washed with 70wt% ethanol and exposed for 20 minutes UV light to sterilize.

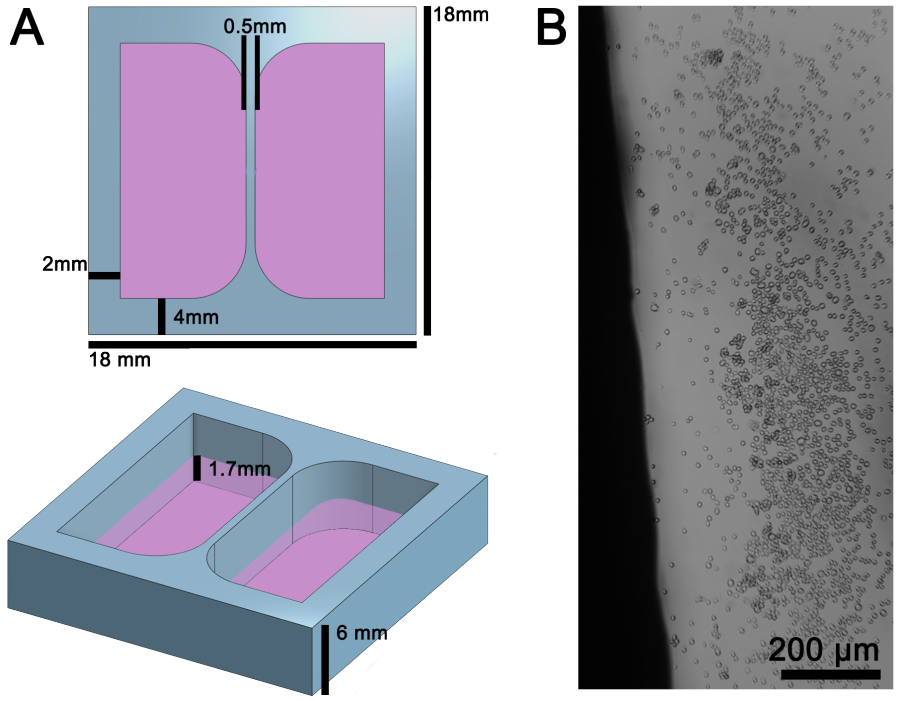

Figure 2.2: [A] Design of the cell excluder. A bounding box that readily fits on top of the patterned glass substrates was used, with a 500 micron split in the middle that creates a cell free zone during cell culture. [B] Cells floating in the medium after being loaded into a well of the cell excluder. Cells grow freely on the exposed substrates, but no cell growth can be found on blocked areas.

Before culturing, excluders were washed with 70wt% ethanol and dried whilst exposed to UV light for 20 minutes to avoid contamination. Then, the excluder devices were placed on top of a thin square glass slide (18 mm by 18 mm) in a six well. Cell excluders were placed such that the cell free zone would align perpendicular to the fiber direction. 200μL of cell medium was added containing $0.3 * 10^6$cells/ml (Figure 2.2.B), and cells were grown to confluency. Then, 24 hours before removal of the cell excluder, medium was replaced with fresh medium containing no FBS to slow cell proliferation. Then, excluders were removed, and the well was filled with 2.5mL of fresh medium. This process is schematically depicted in Figure 2.3. Cells were left to migrate and cover the cell free zone, and the wound width was captured after 0 hours, 6 hours and 12 hours. Average wound width was measured using ImageJ.

Wound healing capability is reported as the wound width at time t (D_t) as a fraction of the initial wound width (D_0):

$$WHC = \frac{D_0 - D_t}{D_0} \tag{2.2}$$

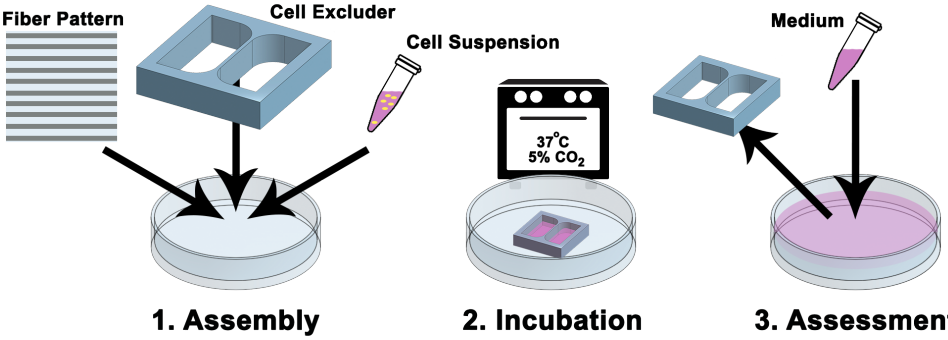

Figure 2.3: Schematic overview of workflow for cell migration experiments using a cell excluder. First, the setup is assembled using a glass slide (either with or without fibers), the cell excluder, and the culture medium with appropriate cell suspension (1). It is then incubated until cells are confluent (3), after which the excluder is removed and fresh nutrient starved medium is added (3). The setup is then ready for observation.

2.2.5. Cell Shape Measurements

Cells were seeded onto fiber patterned substrates and the control at a density of $0.3 * 10^4$cells/ml. Then, cells were left to attach for 24 hours. Cell shape measurements were performed on individual cells (no cell-cell contact) by imaging them with phase contrast microscopy using a 40x objective. At least 120 cells per condition were tested. Cell shape analysis was done by cell tracing with ImageJ. Dimensional data from the cell was then extracted and further analyzed in Excel. The aspect ratio is defined as the ratio between the long (B) and short axis (A) of the cell (see Figure 2.4):

$$AR = \frac{A}{B} \tag{2.3}$$

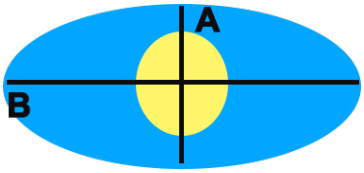

Figure 2.4: The aspect ratio of a cell is given by the ratio between the long axis (B) and short axis (A). A high aspect ratio would indicate elongated cells, and low aspect ratios indicate relatively round, or unpolarized cells.

2.2.6. Cell migration through a Fibrous Membrane

A transwell inspired device was designed to test for the effect of the electrospun fiber composition on the migration of cells through a fibrous network. For this, a device was developed on top of which a fibrous membrane could be electrospun. This way, it allowed for seperation between the cell seeding chamber and well plate medium. The device was printed using the same materials and printing settings as the cell excluder. To create suspended fibers on top of the device, a conductive initiator connected to the grounded collector plate for electrospinning was used. Additionally, the cylindrical chamber of the device was filled with aluminum foil that was directly connected to the grounded plate. To increase the fiber density, fiber spinning was initiated multiple times, but at the cost of precision. Additionally, by rotating the device during the process, fibers can be suspended orthogonally on top of one another, and a fibrous membrane can be created. Three different compositions of the membrane are used for testing. In this way, fibers were drawn in both directions at 15 micron fiber distance. Firstly, a membrane containing fibrinogen fibers (FIB) was used. A membrane containing fibrinogen and gelatin

fibers (FIB-GEL) was created by creating fibrinogen fibers in one direction and gelatin fibers in the other. Lastly, a gelatin fiber membrane (GEL) was used. The average pore size of the membrane was measured using image segmentation via imageJ. Samples were sterilized before cell seeding by exposing to UV light for 20 minutes. Samples were submersed in PBS overnight at 37°C before cell culture.

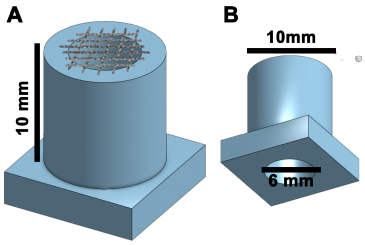

Figure 2.5: [A] Bottom view of the design of transwell design. [B] Top view of the design. Cells can be seeded within the cylindrical chamber and observed to migrate through the membrane.

To prevent cells dropping directly through the membrane during cell seeding, a fibrin gel containing cells was prepared on top of the membranes following adaptation of established protocols [44, 45]. For this, a 7mg/ml solution of fibrinogen dissolved in PBS was prepared. Then, a thrombin solution of 5U/ml was prepared by dissolving thrombin powder directly in PBS. Cells are suspended in the fibrinogen solution down to a concentration of $0.2 * 10^6$cells/ml, and thrombin is added to the solution. 100 μL of the gelling solution is pipetted directly on top of the membranes inside the printed cylinders. As the gel sets, the device is hold steadily against a substrate to prevent the gel leaking through. A gel is formed on top of the membrane within 30 seconds. A control group with no fibrous membrane was prepared by directly letting the fibrin set in the well. Then the wells were plated in a 6 well plate containing 3 ml of cell medium and incubated for 24 hours. After incubation, cells that migrated from the gel were released by trypsin treatment. Shortly, after incubation, the membranes were washed with PBS and then transferred to wells containing 1mL of trypsin and incubated for 5 minutes. Then, cells in the trypsin solution were counted using a hemacytometer. The number of cells were noted as the number of cells migrated relative to the seeding density. These steps are schematically shown in Figure 2.6.

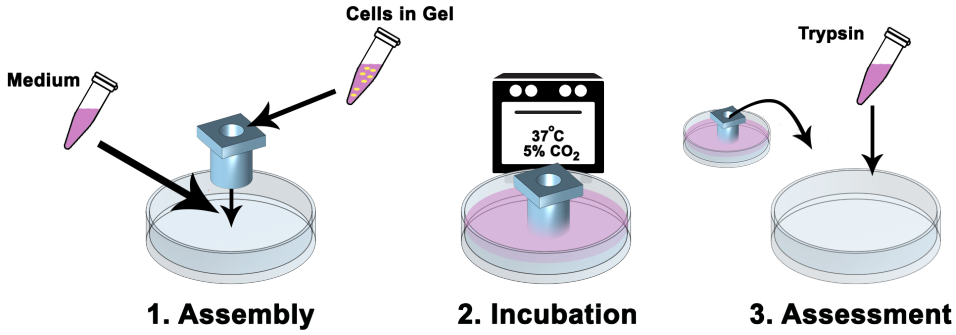

Figure 2.6: Schematic workflow for testing cell migration through the fibrous membrane. The cel suspension is added on top of the membrane and incubated for 12 hours. Then, cells at the bottom of the membrane are trypsinized and counted using a hemacytometer.

2.3. Statistical Significance

All experiments used to test for statistical significance were performed in triplicates (n=3). Significance between groups was tested using an unpaired student t-test, and significance is reported only when a p-value≤0.05 was obtained. Statistical significance is indicated graphically with an asterisk (*).

3

Results

3.1. Electrospinning

3.1.1. Electrospinning Gelatin

Gelatin fibers were prepared using a range of different setup parameters using a 19wt% gelatin solution in a blend of acetic acid and ethyl acetate. Using a voltage between $100V \leq U \leq 200V$ and a flow rate of $12\mu L/hr \leq Q \leq 25\mu L/hr$ straight, parallel fibers can be spun, down to a fiber spacing of approximately 50 μm. At higher fiber densities, fibers start being deposited randomly and precise control is lost. When increasing the voltage ($230V \leq U \leq 320V$), wavy fiber patterns can be deposited. Furthermore, by using higher flow rates ($30/hr \leq Q \leq 50\mu L/hr$), the fibers start containing beads. By further increasing the flow rate, thick fibers can be deposited, and no control can be exerted over the fibers using the voltage.

3.1.2. Electrospinning Fibrinogen

The solubility of fibrinogen in different acidic electrospinning solvents has been tested and qualitatively assessed (Table 3.1). It can be seen that the solubility drops as the concentration of fibrinogen is increased . However, results primarily show that the protein is soluble in PBS at high concentrations (up to 160 mg/ml). Additionally, acetic acid has shown to be a reasonable solvent for fibrinogen.

As the success of electrospinning is aided by the volatility of the solvent, it was attempted to electrospin 100 mg fibrinogen solved in different blends of acetic acid and PBS. A description of the fiber morphology of different blends spun at 100 V and a flow rate of 15μL/hr is shown in Table 3.2. Generally, the addition of acetic acid causes the solution to be more viscous and electrospun fibers with higher concentrations of acetic acid showed bead formation. Furthermore, it was found that electrospinning of fibrinogen using a PBS-acetic acid blend consistently led to gel formation at the nozzle.

Moreover, similar control over fiber morphology as with gelatin can be exerted by changing the electrospinning parameters (Figure 3.1). When using a blend of 3:1 PBS and acetic acid to solve 100 mg of fibrinogen, straight fibers can be spun in the voltage range of $80V \leq U \leq 140V$. Voltages above 200V and up to 300V shows the steady formation of wavy fibers. Similarly as with gelatin, increasing the flow rate ($20\mu L/hr \leq 35\mu L/hr$) leads to bead formation. However, a further increase of flow rate did not lead to thick fiber depositions. Instead, the solution started flowing freely with no fiber formation.

Table 3.1: Qualitative evaluation of solubility of fibrinogen in electrospinning solvents.

Fibrinogen (mg/ml)	Water	PBS	Acetic Acid	Ethanol
60	+/-	+	+/-	-
120	-	+	+/-	-
160	-	+	-	-

Table 3.2: Table containing the results of fiber morphology of electrospun fibrinogen using different ratios of PBS and Acetic Acid. Fibrinogen is dissolved at 100 mg/ml, and electrospinning is done at 100V and a flow rate of 15μL/hr.

PBS	Acetic Acid	Fiber Morphology
1	1	Beaded
1	2	Beaded (Inconsistent Deposition)
2	1	None
3	1	Straight
4	1	Straight (Inconsistent Deposition)

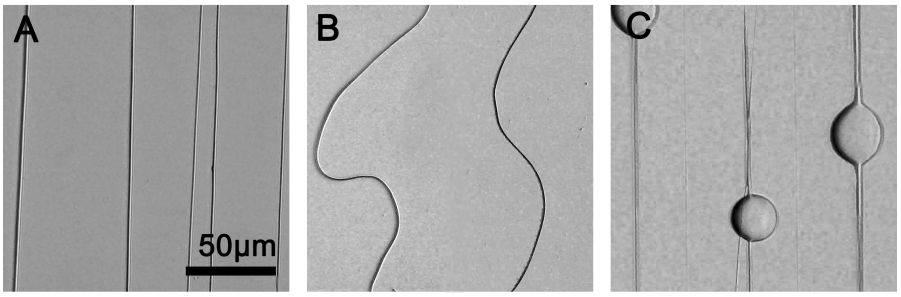

Figure 3.1: Morphology of fibrinogen fibers under different conditions. [A] Straight fibers (U=100V, Q=12μL/hr). [B] Wavy fibers (U=230V, 12μL/hr). [C] Beaded Fibers (U=100V, Q=35μL/hr).

3.1.3. Chemical Characterisation of Fibers

In order to characterize the effect of electrospinning on the final protein structure of gelatin and fibrinogen, an FTIR spectrum of pulverized fibers was recorded and compared with their respective unprocessed powders. First, the FTIR spectrum of gelatin powder and gelatin fibers is shown in Figure 3.2.A-C. Second, the FTIR spectrum of fibrinogen powder and fibrinogen fibers are shown in 3.2.D-F. Clearly, the presence of the Amide A band (3300cm^{-1}, green) attributed to N-H stretching can be found for all cases. Additionally, the Amide I band (1650cm^{-1}, blue) and Amide II band (1550cm^{-1}, red) can be recognized for both gelatin and fibrinogen powder and electrospun gelatin and fibrinogen fibers. These are related to the C=O stretching mode and N-H bending mode respectively. Whereas the spectra of electrospun gelatin and gelatin powder are near identical, a clear shift of the Amide I band peak (Figure 3.2.F) can be found towards lower wavelengths. Lastly, the Amide III shows little change before and after electrospinning for both proteins.

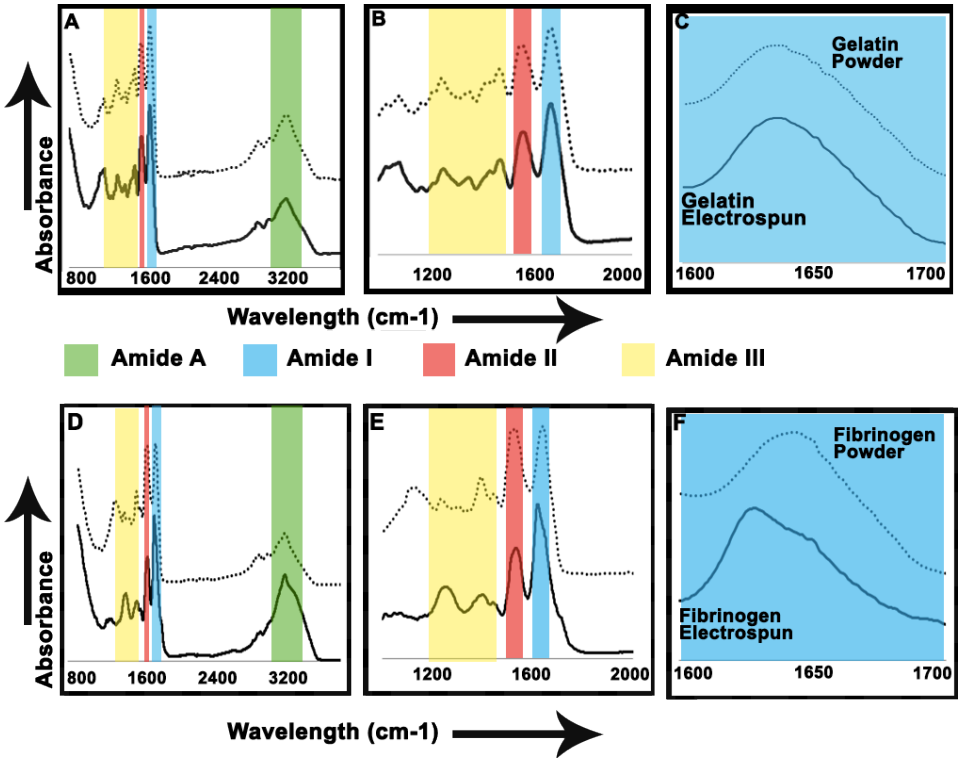

Figure 3.2: FTIR spectrum of gelatin [A,B,C] and fibrinogen [D,E,F] before (dotted line) and after (continuous line) electrospinning. Even after electrospinning, the protein shows the intactness of many characteristic protein bands. [A,D] Full recorded spectrum. [B,E] Close up on several amide bands. [C,F] Close up of Amide A band. Green: Amide A band. Blue: Amide I band. Red: Amide II band. Yellow: Amide III band.

3.2. Cell Viability

3.2.1. Sample Preparation

Substrates containing different spacing of gelatin and fibrinogen fibers were created to study cell viability and cellular migration, and are shown in Figure 3.3. Sometimes, fiber drawing was not initiated properly causing either missing or additional fibers, but final spacing between fibers was relatively consistent with the programmed spacing.

Cells were seeded on substrates containing different amounts of fibrinogen or gelatin fibers. Cells were counted 24 and 48 hours after seeding. Figure 3.4.A shows the number of cells per square cm at these time points per substrate. It can be seen that cells steadily grow on all substrates, as a significant difference can be found between 24 and 36 hours in all cases. However, no significant difference in cell growth can be found between different substrates. Figure 3.4.B shows the relative viability of the cells as a fraction of the cell count on control. Indeed, it seems that cell viability is not altered significantly due to the additions of gelatin or fibrinogen fiber patterns.

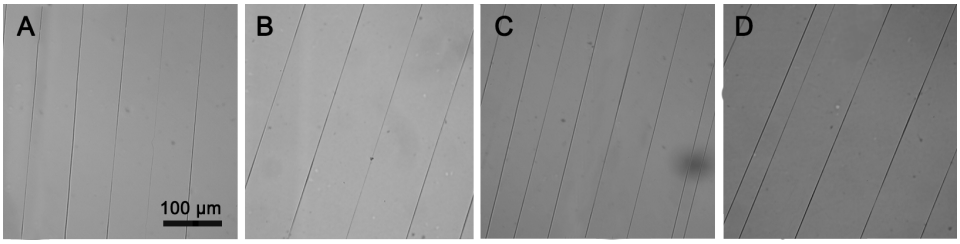

Figure 3.3: [A,B] Substrates containing fibrinogen fibers (FIB60 (68±14μm spacing) and FIB120 μm (129±19μm spacing) respectively). [B,D] Substrates containing gelatin fibers (GEL60 (66±9μm spacing) and GEL120 (126±23μm spacing) respectively).

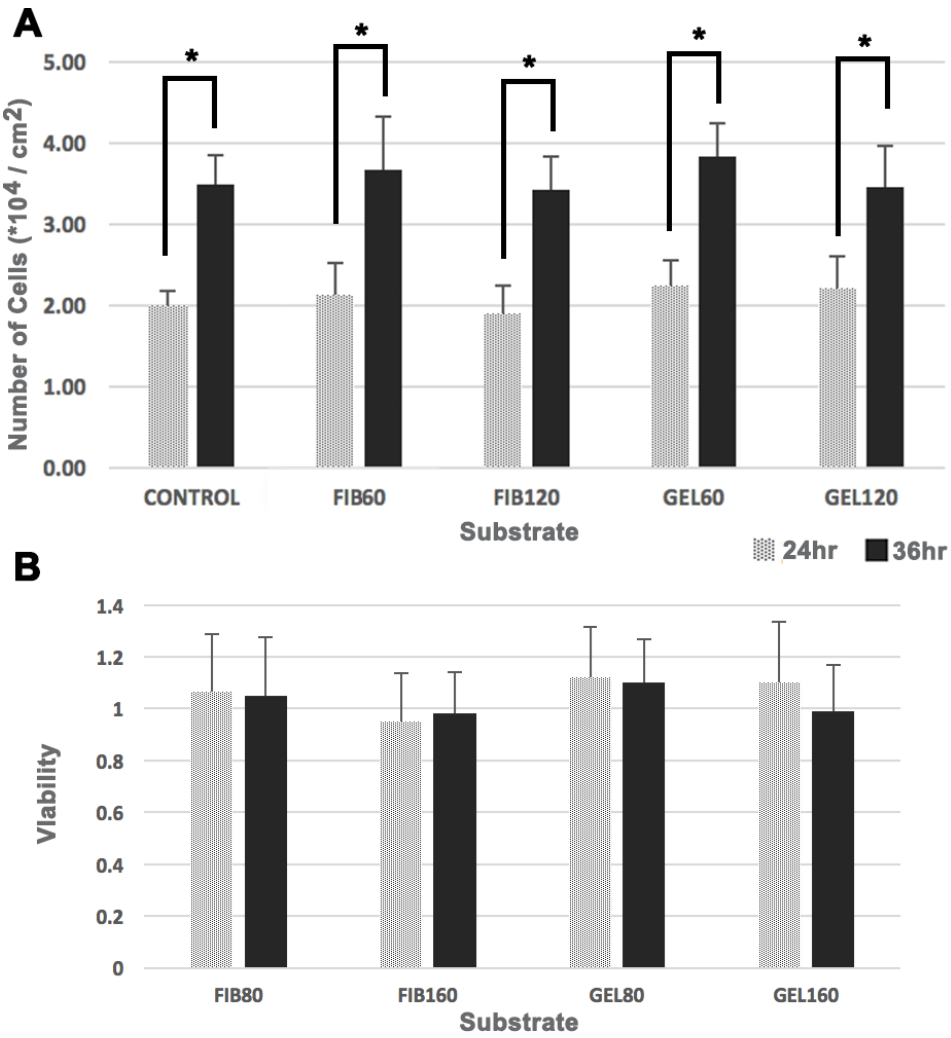

Figure 3.4: Cells grow steadily on all substrates, and there is no difference in viability. [A] Cell proliferation on the different samples. [B] Cell viability of the electrospun fibers when compared to the control. It can be seen that cell viability is not significantly altered between the different substrates. Statistical significant differences are indicated with an asterisk (*) ($p \leq 0.05$).

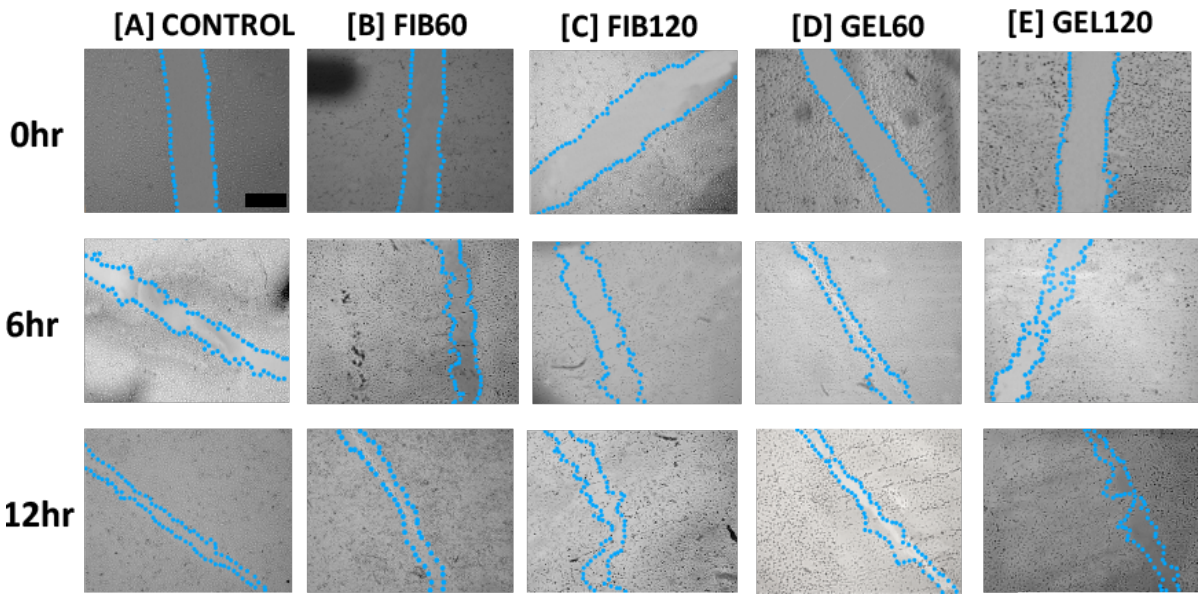

Figure 3.5: Microscope images of the wound width after creation of a 500 micron cell free zone at 0 hours, 6 hours and 12 hours on [A] control substrate. [B,C] Substrates with fibrinogen fibers (60μm and 120μm spacing respectively). [D,E] substrates with gelatin fibers (60μm and 120μm spacing respectively). Scale bar (top left) indicates 500 μm.

3.3. Cell Exclusion Assay

In vitro wound healing assays were studied on substrates containing different amount of electrospun fibers. Phase contrast images were taken of the samples directly after removal of the cell excluders, and after 6 hours and 12 hours (Figure 3.5). Additionally, a graph of the wound healing capacity on different substrates is shown in Figure 3.6. No additional time points were taken as cells completely covered the surface overnight.

First, it can be seen that the cell excluders were successful in creating a cell free zone of approximately 583±65 μm on unpatterned surfaces. Additionally, the cell excluders were effective in selectively blocking cell growth, even on patterned substrates. No significant difference was found in the wound width of the control and the FIB60 (577±82μm), FIB120 (594±75μm), GEL60 (597±64μm) and GEL120 (559±69μm) substrates. Furthermore, the initial wound width showed no significant difference between the fiber patterned substrates. After 6 hours, the cell free zones were shown to be partially covered on all substrates. Clear visual differences in the pattern of wound healing can be observed on fiber patterns as opposed to non-fiber patterns. For example, the wound edges appear to be more irregular (jagged) when fibers were present. Small sections of the cell free gap were already covered with cells after 6 hours on substrates containing fibers, whereas cell sheets on the control did not show this behaviour. Furthermore, on fiber substrates, it can be seen that cells readily split off from the cell sheet and migrate individually towards the other wound edge (Figure 3.7.A-B). After 12 hours, the cell sheet shows tongue like growths covering the initial cell free zone along the fibers (3.7.C). After this, the rest of the cell sheet followed to cover the substrate fully. As such, whereas a general increase in wound healing capacity can be found on all substrates containing fibers, an increase in fibers was associated with increasing gap closure rates. However, it should be noted that a significant difference of wound healing capacity was found only between the control with the GEL60 substrates.

3.4. Cell Polarization

As such, even though in most cases a significant change of cell migration could not be observed, fiber substrates clearly showed two distinct modes of cell migration: both sheet migration (Figure 3.7.A) and single cell migration (Figure 3.7.B) could be observed. This was in contrast to a single mode of cell migration (sheet migration) on the control substrates.

To investigate the direct effect of the different fiber substrates on the migration potential of cells, a low density of cells was seeded onto the substrates and their aspect ratio was measured after 24 hours. On unpatterned substrates, cells often spread out, showing a relatively low aspect ratio as seen

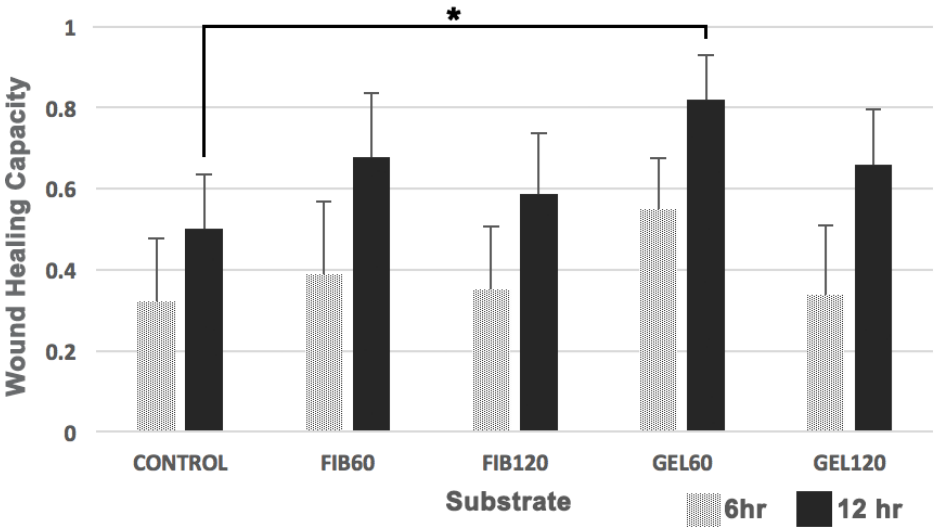

Figure 3.6: Average wound healing capacity expressed as a ratio of wound width at a given time point and the original wound width. Statistically significant differences are shown with an asterisk (*) ($p \leq 0.05$).

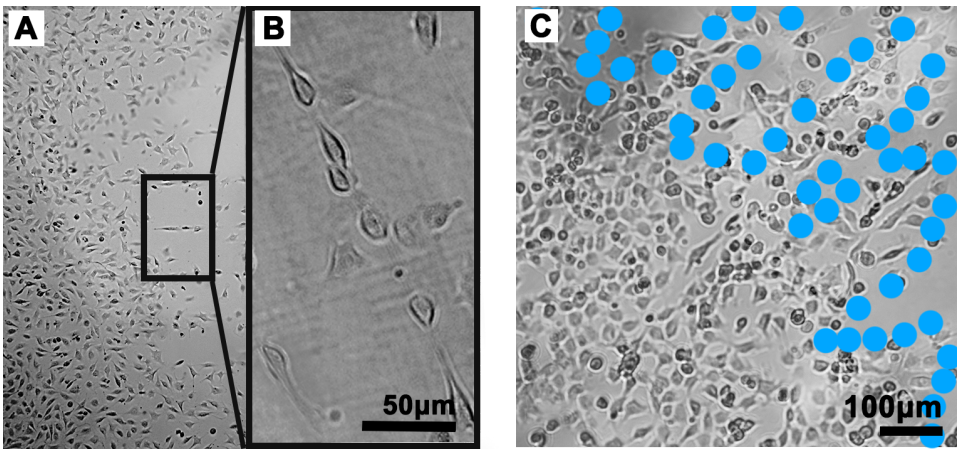

Figure 3.7: Closer looks at cell migration along fibers. [A] Wound edge after 6 hours. [B] Cells traveling along the fibers. It can be seen that the fibers are used a cellular ”highways”. It can be seen that cells split from the cell sheet to migrate individually towards the other wound edge. [C] Tongue like outgrowths (outlined with blue) from the cell sheet during wound healing are common on fiber patterns.

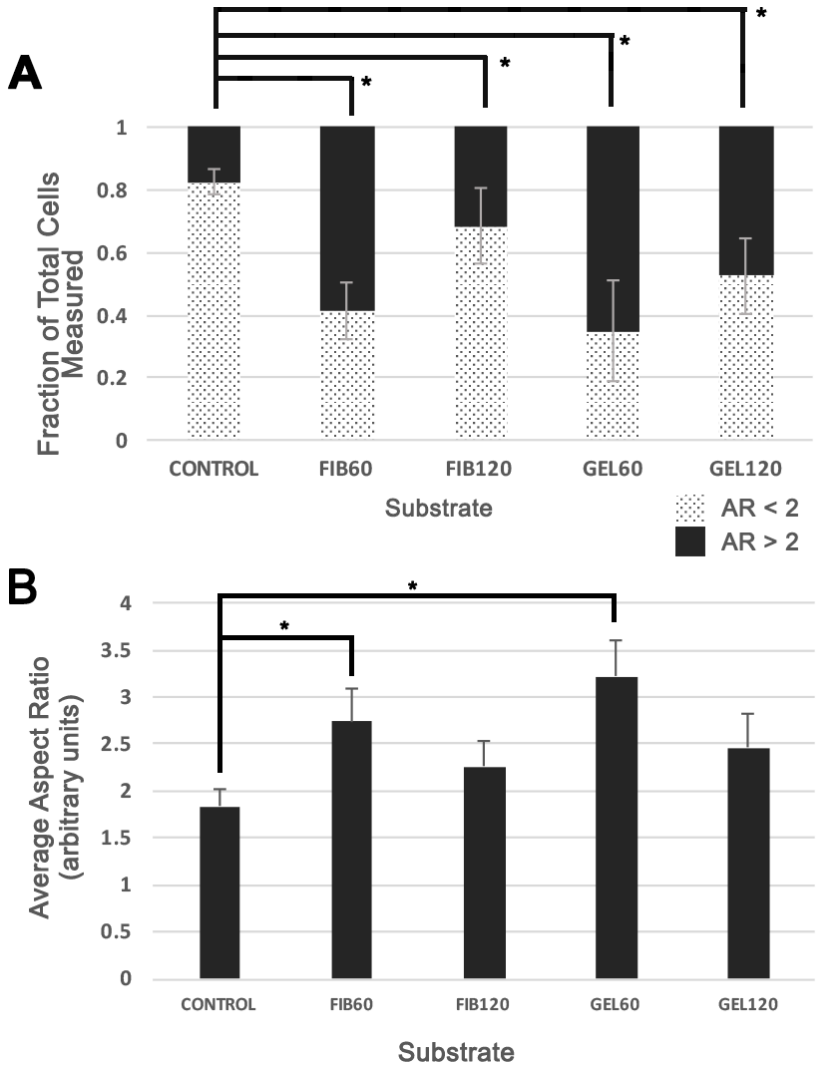

Figure 3.8: Aspect ratio of cells found on the different substrates. [A] Cell with relative low aspect ratio on a flat substrate. [B] Higher aspect ratio cell attached to a fiber, but with protrusions onto a flat substrate. [C] High aspect ratio cell completely attached to a fiber.

in Figure 3.8.A. Cells attaching partially to fibers and partially to the flat substrate showed a more elongated morphology, such as seen in Figure 3.8.B, whereas cells attaching to fibers only showed the highest amount of elongation. Figure 3.9.A gives the relative fraction of cells found on the substrates with high aspect ratio (AR>2) and low aspect ratio (AR<2). Figure 3.9.B shows the average aspect ratio found on the substrates. It can be recognized that the all fiber patterned substrates showed a significant increase of polarized cells as a fraction of all counted cells. Indeed, both the FIB60 and GEL60 substrates had more than 50% of cells counted with a polarization higher than an aspect ratio of 2. At the same time, only the FIB60 and GEL60 substrates showed a significant increase of the average cell polarization on the substrates when compared to the control. Indeed, as the fiber density increases, it is relatively easier for cells to encounter and attach to fibers. This increase in average aspect ratio, together with the increase in number of polarized cells notes that cells have higher migratory potential along fibers, which agrees with the increases in wound healing for both FIB60 and GEL60.

3.5. Cell Migration through a Fibrous Membrane

The cell exclusion assay allowed the investigation of sheet migration, and showed increased wound closure rates on fiber patterns. To further assess the effect of fiber composition on cell migration a transwell-inspired design that makes use of orthogonally aligned fibers to create a porous 2D scaffold

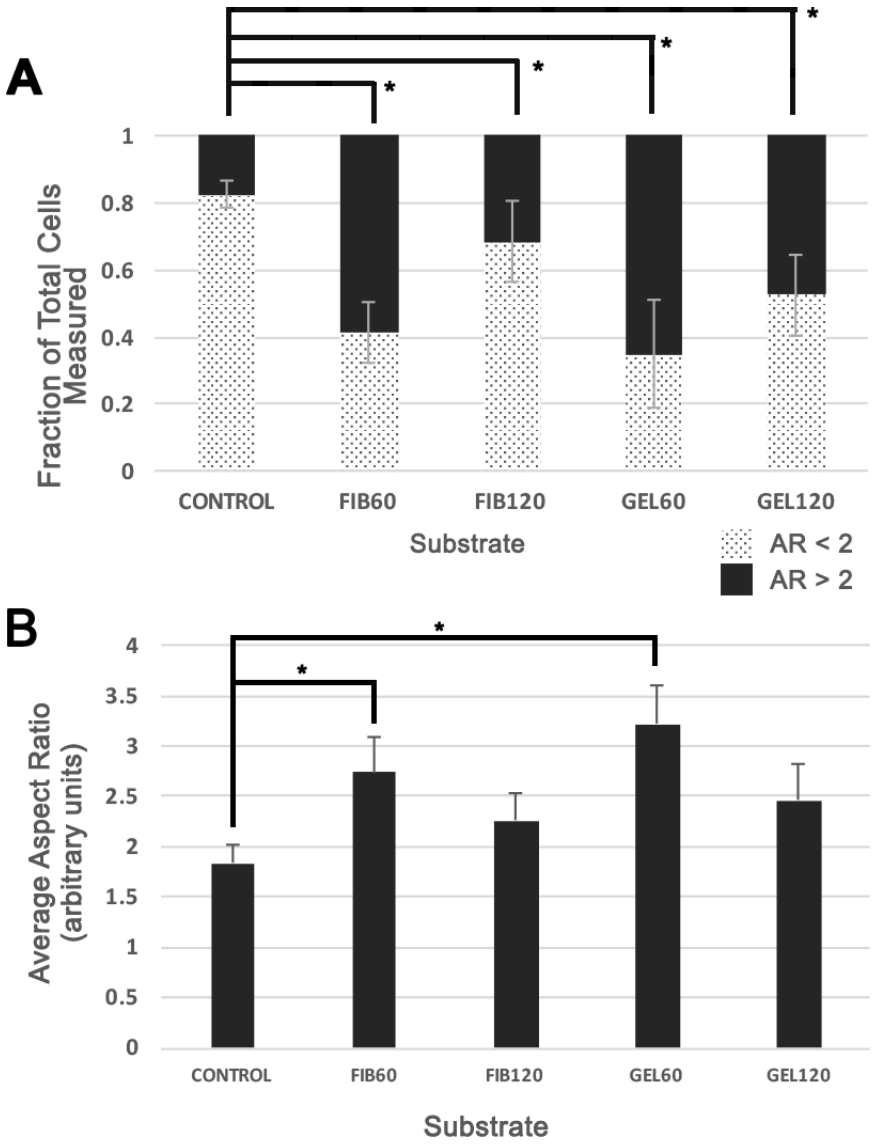

Figure 3.9: [A] Fraction of cells with low (AR<2) and high aspect (AR>2) ratio. Note that all fiber samples contain cells with a relatively high aspect ratio. [B] Average aspect ratio of cells on different substrates. Note that the aspect ratio is significantly larger on substrates with larger fiber density, as cells find and in turn attach to fibers easily. Statistical significance is indicated with an asterisk (*) ($p \leq 0.05$).

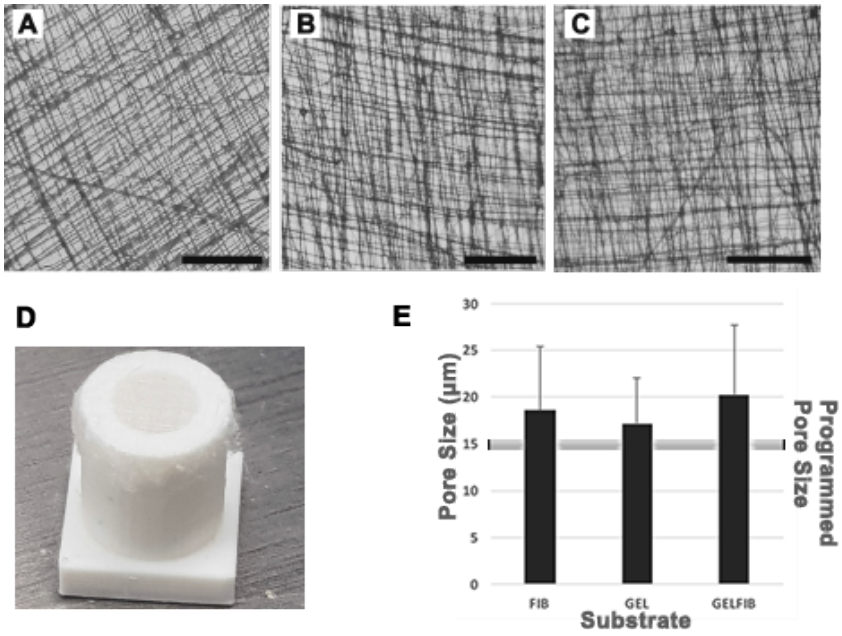

Figure 3.10: [A,B,C] Electrosun fiber membranes of Fibrinogen, Gelatin and Fibrinogen-Gelatin composite membranes. Scale bars indicate 500μm. [D,E] Transwell device design and device after electrospinning. [F] Pore size of the fiber membranes, the line indicates the programmed pore size.

is used.

Fiber drawing on transwell based substrates was more complex, as it required electrospinning on an irregular object. By modifying the electrospinning equipment to use elevated conductive mechanical initiators, drawing of suspended fiber patterns was possible on top of 12 mm high pillars (Figure 3.10). However, during the drawing process, some difficulties presented themselves. As fibers were individually drawn, previously suspended fibers were sometimes ripped away during the drawing of orthogonal fibers. Nevertheless, fibrous membranes were electrospun of both gelatin and fibrinogen, and an alternative network composed of both gelatin and fibrinogen fibers. Figure 3.10.A-C show microscope images of the membranes. Figure 3.10.D shows a photograph of the full device with membrane. Figure 3.10.F shows the pore sizes of the different membranes. The pore sizes are not significantly different from the programmed pore size, nor from one another.

Cell migration after 24 hours was tested from a cell containing fibrin gel, and from a fibrin gel through the different membranes (Figure 3.11). Cells that migrated from the gel were detached using trypsinization. It can be noted that, whereas not significant, the addition of the membranes hinders cellular migration. The cells that migrated from the cells can be clearly seen on the gel alone (Figure 3.11.A), but are hard to distinguish from the fibers directly (Figure 3.11.C-E) on all membranes. Nevertheless, on all membranes, cells can be found attached to the membranes. Cell migration was found to be on slightly larger on samples with gelatin membranes (20±5%) than on samples with fibrinogen (18±6%) and fibrinogen-gelatin composite (16±9%) membranes.

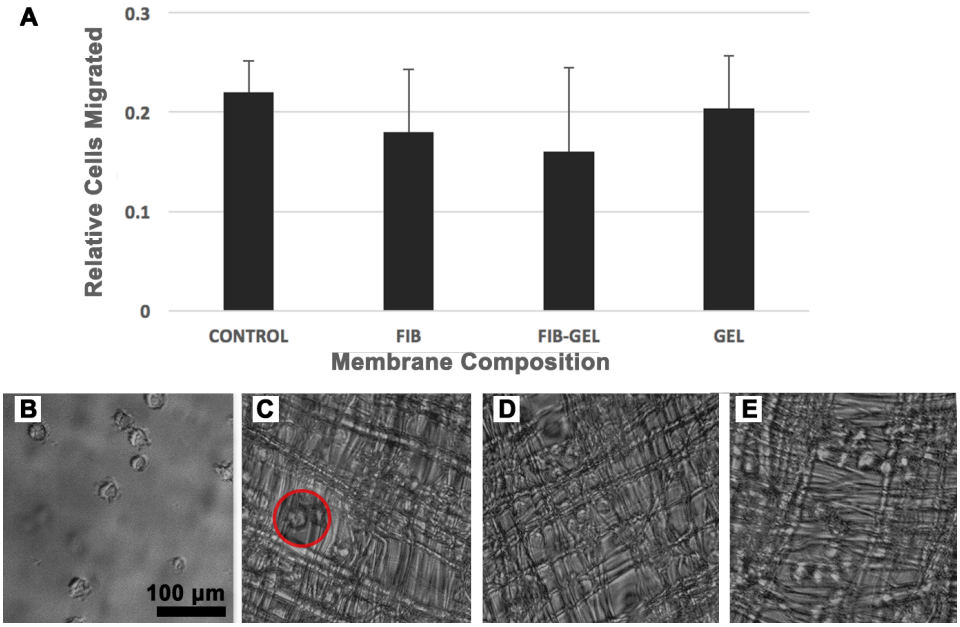

Figure 3.11: [A] Number of cells migrated from the gel after 24 hours relative to the number of seeded cells. Microscope images show cell migration from [B] fibrin gel only, [C] fibrin gel and fibrinogen membrane, [D] fibrin gel and fibrinogen-gelatin membrane, [E] fibrin gel and gelatin membrane. For clarity, a cell on the membrane is encircled.

4

Discussion

4.1. Electrospinning Fibers to Mimic the Early Fracture Environment

The properties of electrospun fibers depend on a wide range of process parameters. By tuning these parameters, some degree of control can be exerted on the resulting fibers [6, 46]. These influencing factors fall into three main categories: setup variables, solution properties and environmental conditions. Setup variables include the flow rate of the supplied polymer solution, the applied voltage, the needle shape through which the solution is ejected, the distance between the needle and collector, and the composition and motion of the collector. These are most easily controlled during the electrospinning process. Solution properties include (but are not limited to) the used molecular weight of the polymer, its concentration and solution viscosity, the solution conductivity, the surface tension. It is difficult to isolate the effect of solution properties on the electrospinning process, as they are heavily interrelated. The environmental conditions include amongst others the temperature, humidity and are often the hardest to precisely control, but can significantly affect the fiber spinning process. In this study, we have shown that fiber properties during low voltage electrospinning can be tuned by changing both setup parameters and solution composition. First, when electrospinning fibrinogen, the use of higher concentrations of saline solvent (PBS) over acidic solvents showed a general decrease in viscosity of the electrospinning solution. This is primarily caused by ionic charges in the saline solution that shield electrostatic attractive forces between protein molecules. Additionally, an increase in ionic charges in the electrospinning solution decreases fiber thickness as the solvent jet experiences larger electrostatic forces during spinning [37]. Second, the use of higher voltages causes instability of the polymer jet during travel, created wavy fiber patterns. Third, a high flow rate causes less evaporation of the solvent, causing the formation of thicker beaded fibers. Similar results with electrospinning fibers have been previously observed [6, 37]. However, no further characterization of the structural fiber properties has been done (i.e. characterization of the fiber thickness and surface morphology). Differences in these properties can alter ECM interactions with cells [41], and further studies are encouraged to apply characterization techniques to compare differences between the structural properties of gelatin and fibrinogen fibers.

On the other hand, using FTIR spectroscopy, some chemical characterization is performed. It has been shown that the use acetic acid and low voltages allows for electrospinning of gelatin and fibrinogen fibers without significantly changing the distinctive protein characteristics of the used biopolymers. However, it should be noted that the Amide I peak of electrospun fibrinogen shows a significant shift towards lower wavelengths, indicating an increase of β-sheets [47]. This agrees with the observation that fibrinogen solved in acetic acid clots easily during electrospinning, as $\beta-$sheets promotes intermolecular bonds [48]. Furthermore, it agrees with similar observations made in the structural change of collagen during electrospinning [49]. Acetic acid molecules are likely to reconstruct hydrogen bonds, partially disrupting hydrogen bonds between amide and carboxyl groups that primarily constitute the α-helix structure.

Recently, Mirzaei-Parsa et al. [50] has shown a similar use of acidic solvents electrospinning fibrinogen. They have used a blend of acetic and formic acid, and performed FTIR on the electrospun fibers,

showing a smaller change in the Amide I peak. Additionally, they found that for larger concentrations of acetic acid, fiber thickness increased. This agrees with the formation of beaded fibers in this study with larger concentrations of acetic acid. Nevertheless, it has previously been shown that even after changes in the secondary protein structure, fiber properties are still strongly representative of the original protein [49, 51]. As such, the fibrinogen and gelatin fibers are used to reflect the fibrinogen-like (hematoma) fibrous matrix and gelatin-like (soft callus) matrix during fracture healing respectively.

4.2. Cell behavior on Fiber Patterns

As such, in this study, we have investigated the response of endothelial cells to different biopolymer fibers that reflect the early fracture healing environment. First, substrates were patterned using fibrinogen and gelatin fibers to reflect the inflammatory and soft-callus phase during bone fracture healing. The substrates were patterned using inter-fiber distances of 60μm and 120μm to allow for assessing both the effect of (chemical) fiber properties and overall fiber patterns. Second, cell viability was assessed over 48 hours of culturing on the different substrates. As a control, unpatterned glass substrates were used. As such, no significant differences were found for the cell viability, neither between different types of fibers and different fiber spacing. Instead, cells grew steadily on all substrates, showing significant differences between cell count at 24 hours and 48 hours after seeding. Indeed, it has previously been shown that differences in surface patterns do not alter the proliferative ability of cells at such time scales [52, 53]. It should be noted, however, that these studies have applied different cell types for culture. Nevertheless, similar behavior can be expected. On the other hand, the composition of surface has been previously shown to significantly affect the viability of cells. For example, Relou et all. [54] cultured endothelial cells on both gelatin and fibrinogen coated culture dishes, and noted a significant increase in cell growth when compared to uncoated substrates. Moreover, cell growth seemed to be significantly larger on gelatin coated substrates than on fibrinogen coated. These differences between the results of coated surfaces versus the patterned surfaces can be explained due to the total culture surface that is covered by protein: whereas during coating most of, if not all of, the surface is altered, the use of nanofiber patterning allows for only partial coverage of the surface with protein. In other words, we theorize that the use of denser biopolymer fiber patterns that cover a larger amount of surface area, would result into a difference between cell viability on fiber patterned substrates and unpatterned substrates. This hypothesis is supported by the general, although not significant, increase in cell viability with denser fibers at both time points.

During fracture healing, there is a continuous need of cellular migration towards the fracture site [12]. Moreover, the composition of the early fracture micro-environment has shown to significantly alter cell behavior and determine the outcome of fracture healing [21, 55]. As such, the effects of fibrinogen and gelatin fiber patterns on the wound healing capacity of endothelial cells have been studied. Additive manufacturing was used to fabricate designs that allow for selective cell growth, effectively creating a cell free zone onto which cells could readily grow. Similar devices and patterning methods have been applied by others to create a cell free zone, either by directly removing cells via chemical, mechanical or electrical means [42], soft lithography [56], and removable parafilm strips [57]. However, these techniques often show to either cause irregular wounds, require a large amount of manual handling, or are time costly and involve a complex manufacturing process. By using additive manufacturing, cell exclusion devices can be easily tuned to the needs of the culture and study, with minimal intervention and manual handling needed during fabrication. The design used in this study can be used to culture cells with a cell free zone of 583 ± 65 μm on flat, unpatterned substrates. Cell free zones were effectively created on unpatterned substrates, and substrates containing fibrinogen and gelatin fibers at different spacings. The cell free zone was aligned orthogonal to the fiber direction to simulate cell migration along the fiber patterns.

Wound healing capacity has been expressed as the wound width at 6 hours and 12 hours relative to the initial wound width. First, a general increase in wound healing capacity was found for all fiber patterns as compared to the control, and was higher on gelatin patterns than on fibrinogen patterns with the same spacing. Second, it has been shown that gelatin fibers at 60 μm fiber spacing significantly caused an increase in wound healing capacity. This result is in line with previous studies that show an increase in wound healing capacity of MG-63 cells on micropatterns orthogonally aligned with the cell free zone [53]. Additionally, wound healing capacity of different cell types have been previously shown to slightly increase on gelatin coated substrates over fibrinogen coated substrates [58].

Similarly, Chen et al. [58]. showed a general but not significant increase of wound healing capacity on substrates containing gelatin and fibrinogen over uncoated control substrates. However, the increase in wound healing capacity is unlikely related to differences between cells proliferation rate on the different substrate, as cell viability generally did not differ much across samples. Instead, a different phenomenon was recognized on substrates containing fiber patterns. Whereas most fiber containing substrates did not significantly improve the average distance between wound edges, single cells were found to migrate along fibers to populate the cell free zone after splitting off from the cell sheet, as depicted in Figure 4.1. After this, tongue like outgrowths from the cell sheets can be found covering the cell free zone along the fibers. Only then does the rest of the cell sheet follow.

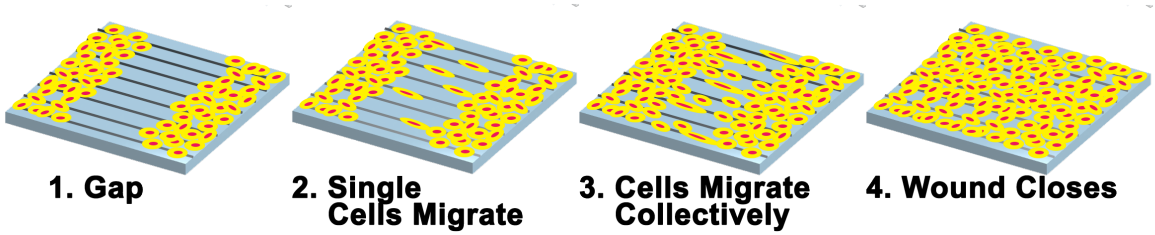

Figure 4.1: Cell migration onto a cell free zone as found on fiber patterns. After removal of the cell excluder (1), cells attached to fibers singularly migrate into the cell free zone along the fibers (2). After this, the cell sheet first covers the area along which the fibers lie with tongue like outgrowths (3). The complete cell sheet then follows to cover the full zone that was initially cell free (4).

Previous studies have shown the capability of cells to individually align with and migrate along single fibers. Estabridis et al. [40] showed that glioblastoma cells attached to suspended single fibers to migrate along them. Using single suspended fibers, Sharma et al. [59] showed similar behavior in fibroblast cells. They had shown that cells split from the cell sheet to migrate seperately along the suspended fibers. At later timepoints, the cell sheet followed after depositing new ECM that could support sheet migration. However, some key differences between their study and this one are that their model did not allow for sheet migration directly, as there was no supporting ECM present. Indeed, fibrous fracture tissues are often dense enough to support migration of interconnected cells [55]. As such, we argue that the use of fiber patterned substrates more closely reflects endothelial cell migration in vivo.

Cellular migration is known to be paired with changes in cellular morphology [5]. Before migration, cells take on a more elongated morphology that assists locomotion. As such, the influence of fibrinogen and gelatin fibers and fiber spacing on the polarization of cells is observed. It was found that the fraction of polarized cells is significantly increased on both fibrinogen and gelatin fibers at a fiber spacing of 60 μm when compared to flat substrates. Using semi-aligned electrospun PLGA fibers, Ahmed et al. [41] showed similar behavior of endothelial cells, observing alignment of the cells parallel to the fibers. Additionally, similar fiber patterns have shown cells to elongate along the fiber tracks before cell migration [59]. In general, gelatin fibers showed a larger fraction of polarized cells than fibrinogen. It has been shown that the growth of new vessels in damaged tissues follows the elongation of vascular cell migration [60]. As such, the observed increase in the fraction of elongated cells on gelatin fibers is reflective of the angiogenic potential of the soft callus in fracture healing. Indeed, other in vitro studies have shown the increased viability of gelatin gels/coatings over fibrin gels/coatings to support vascular cell migration [58, 61].

Overall, it can be said that the cell viability is not significantly altered by the addition of fiber patterns. However, an interesting phenomenon arises when fibers are present, likely driven by the competition between cell adherence to the glass substrate and the fibers. As the fibers consist of natural polymers, the fiber surfaces directly present binding sites that cells prefer over the glass substrates [27]. This is supported by the fact that cells can be seen in this study to individually polarize and migrate on and along the fibers. However, it has previously been shown that cells bind more easily to fibrinogen than gelatin [62]. As such, for cell migration driven by the availability of cell binding sites alone, it is expected that fibrinogen fibers would increase the migratory potential of cells. On the other hand, mechanical properties of the substrates have been shown to significantly influence cell migration [32]. It has

previously been shown that collagen and gelatin fibers have a stiffness much higher than fibrinogen fibers [63, 64]. In other words, this means that cells can exert much higher forces on gelatin fibers as opposed to fibrinogen fibers, and thus migrate more easily. In contrast, on first sight this also indicates that cells would more easily migrate glass, as it is the stiffest substrate. However, the glass substrate primarily shows intactness of the cell monolayer and as such primarily shows cell sheet migration. It has been shown that the cell-cell junctions cause retardation of overall cell migration [65]. This is because in the case of cell-cell junctions, another force which opposes the direction of migration arises. In other words, as opposed to cell-substrate binding, the forces of cell-cell junctions play an antagonistic role in the migration of the cell sheet. As such, because the binding sites of fibers allow the detachment of single cells from the cell sheet, overall cell migration and wound healing capacity is increased.

4.3. Cell Migration Through a Fibrous Matrix

Furthermore, to investigate cell migration through a fibrous matrix reflective of the early fracture environment, a transwell inspired device is developed. Simply said, a fibrous membrane is electrospun on top of a 3D printed open cylinder. Similar approaches have been previously taken to create electrospun membranes on top of transwell devices [66, 67]. However, these studies often involved much manual handling of the membranes, making the process unreliable, with much variation between samples. On the other hand, most of these studies have created membranes with smaller pore sizes (down to 0.5 μm), which is more reflective of the pore sizes of the fracture tissue as found in vivo [55]. Nevertheless, the migration studies here show that the fiber structure influences the migration of cells. In general, a decrease is found in cell migration on all membranes when compared to control. Due to the fibrous composition of the membranes, it was expected that the increased relative surface area that contains cell binding sites would increase cellular migration. However, it is likely that, when compared to control, the added physical constraint of a membrane instead impedes migration. Whereas not significant, a slight increase in cell migration was found on the gelatin membrane when compared to the other membranes. Similarly as on the fiber patterned substrates, this is likely caused by the higher stiffness of gelatin as compared to fibrinogen [63]. On the other hand, the results indicate that the physical constraints imposed on the cell migration have a higher influence than the composition of the fibers. Along the same lines, geometrical and physical constraints have previously been shown to strongly direct cell behavior [41, 68].

4.4. Model Relevance and Limitations

The fracture environment is composed of fibrous tissue that is remodeled from a fibrin laced clot to a more collagenous soft callus [12]. During the fracture healing process, cells continuously migrate into the fracture site. Furthermore, it is known that the structural properties and composition of the involved scaffolds can influence cell fate and migration [5, 15]. The use of electrospinning to create fiber patterns has recently gained popularity as an ECM analogue to study cell behavior in vitro [40, 41].

This study has integrated the use of a novel electrospinning technique to mimic the effects of the early fracture composition on (endothelial) cell migration. Gelatin and fibrinogen fibers were electrospun using acidic solvent systems. Such acidic solvent systems are known to preserve the major properties of biopolymers [49]. This way, the fibers allow studying cell-matrix interactions as found in vivo.

First, the results of this study show that the addition of fibers on substrates more closely mimic vascularization as found during fracture healing. On fiber patterns, cells emerge singularly from the cell monolayers and migrate into the cell free area, resembling cell migration before vasculogenesis as found in vivo [5]. Furthermore, overall wound gap healing was found to increase on fiber pattern substrates, indicating the role of fibers in directing cellular migration of interconnected cells, which is a process that resembles angiogenesis [5]. Moreover, this study has shown not only the effects of a fiber structure in guiding endothelial cell migration, but the role of fiber composition as well. Indeed, endothelial cell migration was found to be largest on gelatin fibers, which is reflective of vascularization during the soft callus phase in fracture healing [12],

Second, on one the hand, these fiber patterns show to be a reliable representation of the fibrous micro-environment. On the other hand, they are also a simplification of the in vivo situation. The largest difference is that the first proposed model in this study is primarily two dimensional, whereas

Table 4.1: Some key differences and similarities between early bone fracture healing and the used approaches in this study to resemble cellular migration during these phases. *Early on, random fibers are found in the hematoma, but the tissue is gradually replaced with organized, aligned tissue fibers. **Endothelial cells are used in this study, but the used setup allows for integration of co-cultures. ***Currently not assessed, but possible using cultured cell sheets on fibrous membranes.

	(Early) Bone Fracture	**Fiber Patterned Susbtrate**	**Fibrous Membrane**
Structural Properties	Three Dimensional Random Fibers* Dense Network	Two Dimensional Aligned Fibers Sparsely Spaced	Two Dimensional Aligned Fibers Sparse Network
Mechanical Properties	Soft Tissue	Stiff (Glas) Substrate, Soft Fibers	Soft gel and membrane
Chemical Environment	Dynamic Gradients Range of Growth Factors	No Gradient Only FBS	Diminishing Gradient Only FBS
Cellular Components	Multiple with Crosstalk	Endothelial Cells**	Endothelial Cells**
Endothelial Migration	Vasculogenic Angiogenic During Soft Callus (Gelatin-like tissue)	Single Cell Migration Sheet Migration and Cell Sheet Tongues Highest on Gelatin	Single Cell Migration Not Assessed*** Not Significantly Different

fracture tissue is three-dimensional. It has been shown that the cellular behavior is significantly altered in a 3D micro-environment [69]. The in vivo early fracture tissue consists of a 3D environment made out of densely packed fibers [55]. Additionally, the in vivo ECM fibers are gradually aligned during fracture tissue remodeling, and the early ECM primarily shows an unordered tissue structure [55]. Such a difference in fiber alignment can significantly alter cellular behavior. To illustrate, Whited and Rylander [70] showed a significant decrease in cell aspect ratio and alignment on randomly structured electrospun fibers when compared to (semi-)aligned fibers. Furthermore, the fibers in the cell free zone migration study are deposited directly on glass. Previous studies have shown that the stiffness of both single electrospun biopolymer fibers and biopolymeric gels are significantly lower than that of glass, influencing cell behavior [32, 63]. Endothelial cells have previously been shown to directly prefer substrates with higher stiffness [31], and migrate towards substrates with high stiffness. As such, creating fiber patterns on a hydro gel-like substrate more reflective of the softness of the early fracture environment could be used as a substrate for fiber patterns, leading to significant changes in both cell viability and migratory behavior.

Lastly, the micro-environment of the fracture tissue is a cocktail of biological, chemical, physical and mechanical cues that drive cell migration and activity via a range of interrelated pathways [15]. This study applied a monoculture of endothelial cells to study their migratory properties under the influence of fiber composition and density. On the other hand, cell behavior can be significantly altered when the complexity of the system is increased. As such, an additional model is proposed that allows for studying cell behavior in an environment more reflective of the early fracture tissue. By creating a fibrous membrane that separates the cell seeding area and a cell free area, cell migration can be studied under the influence of nutrient gradients as found during fracture healing [42]. Moreover, by embedding the cells within a gel, the differences between substrate and fiber stiffness are partially reduced, and a more reliable result can be obtained. However, this comes at the cost of requiring a more complex fabrication process. The used methodology in this study for assessing cell migration through the membrane poses some limitations. First, direct trypsinization of the membranes can release cells that have migrated from the gel, but have not yet directly migrated through the membrane. As such, migration out of the gel and migration through the membrane is not directly decoupled in this study. Advanced biological imaging techniques that counter this issue exist, such as fluorescence microscopy [42]. Second, the design used in this study makes use of relatively large pores, whereas pore sizes in vivo are much smaller [55]. Moreover, only single cells are counted and migration of a cell network is not directly assessed. Growth of an interconnected cell layer on top of a denser membrane could be used to assess cell migration from a cell sheet through a fibrous membrane. Overall, after optimization, the used platform can serve as promising platform for studying cellular migration through a network of fibers.

Hence, some key resemblances and differences are identified between the used models and fracture healing in vivo, as summarized in Table 4.1. Nevertheless, the use of fiber patterns and membranes has given insight in the importance of fibers and fiber composition for cellular migration and fracture healing.

5

Conclusion

Bone tissue serves an integral part in the body, such as structural support, organ protection, and mineral homeostasis. Additionally, after trauma, bone has the unique capability to fully regenerate into functional tissue. However, a disturbance in the healing process can cause the development of non-union tissue, in which bone is not properly restored. As such, besides being a large individual burden, hospitalization costs for prevention and treatment of non-union tissue has been shown to pose an incredible socio-economic burden. To develop new treatments that can tackle this problem, a thorough understanding of the bone fracture healing process is required. Currently, it is known that bone healing in vivo is done via a multistage sequential process of inflammation, soft callus formation, hard callus formation and bone remodeling. During these processes, a multitude of cells migrate to and within the fracture under the influence of a range of physical, chemical and mechanical cues. As such, previous studies have shown the importance of the biological, physical, chemical and mechanical properties of fracture tissue and their effects on modulating bone healing. However, the working mechanisms of these elements and the role they play in cell migration, and in turn fracture healing, is not fully understood.

This study applies the use of low voltage electrospinning to create fiber patterns that mimic the in vivo composition of the early bone fracture micro-environment. Fibrinogen and gelatin fibers are used to reflect the natural fibrin scaffold (inflammatory phase) and collagenous scaffolds (soft callus phase) during fracture healing. Control over fiber morphology for both types of fibers was performed by tuning process parameters. Furthermore, both fibrinogen and gelatin fibers were prepared using acidic solvent systems. FTIR spectroscopy has been applied to study the effects of these solvents on protein structure. Whereas no changes were found in the gelatin FTIR spectra before and after spinning, fibrinogen showed an increase in β-sheets paired with a decrease in α-sheets. These changes were likely caused by disruption of hydrogen bonds between amide groups and carboxyl groups in fibrinogen due to the acidity of the solutions, causing partial unfolding of the molecule. Similar behaviour has been found by others in electrospinning collagen fibers using acidic solvents. Nevertheless, even after some change in secondary structure, proteins were previously shown to be still reflective of their original function and properties after electrospinning.

As such, endothelial cells were used for cell culture to model cell migration during early fracture healing. Three different results were concluded from these studies. First, it was shown that neither fiber composition nor fiber spacing altered the viability of cells. Second, additive manufacturing was used to print a cell excluder that allowed for reliable growth of a cell free zone. Subsequently, cells were allowed to cover the cell free zone on different substrates containing different types of fibers and different fiber spacing. It was observed that cells used fibers to split of from the cell sheet and migrate individually along the fibers. After this, cellular tongues were formed of collective cell groups migrating along and close to the fibers. Lastly, cell migration on the glass substrate followed to completely cover the cell free zone. Third, to further investigate the effect of these fibers on cell migration potential, the average polarization of cells was studied on the different substrates by measuring cell aspect ratio. Furthermore, the fraction of polarized cells and non-polarized cells was calculated. It was found that cells polarize along the fiber patterns, which assists cell migration. In this way, fibers were shown to increase cellular migration, and reflect in vivo vascularization by showing single cell migration (vasculogenesis) and cell

sheet migration (angiogenesis). Furthermore, differences between cellular migration on fibrinogen and gelatin fibers have shown the importance of fiber, and in turn scaffold, composition. Fibrinogen has been previously shown to contain superior properties for cell attachment due to a larger number of available binding sites. Nevertheless, migration was largest on gelatin substrates, likely due to higher stiffness of gelatin fibers. High stiffness promotes cellular migration as cells can exert higher forces during migration.

Additionally, to further investigate the direct effect of the tissue composition on cell migration, suspended fiber membranes of fibrinogen only, gelatin and fibrinogen, and gelatin only were electrospun on top of a transwell-like device. A cell-laden fibrin gel was deposited on top of the membranes to prevent cells from dropping through the membranes. It was found that all types of membranes significantly impeded endothelial cell migration from the fibrin gel. Furthermore, differences between cell migration on different membranes were minor, and not statistically significant. As such, it was evident that physical restriction posed by the membrane were more relevant in determining cellular migration than membrane composition.

In conclusion, the use of fiber patterns has shown the importance of both the microstructural properties of early fracture tissue (i.e. fibers as opposed to no fibers), and the composition of the tissue (i.e. the early fibrin clot as opposed to the gelatin-like soft callus) as a regulator of cell migration behaviour. Nevertheless, there are some key differences between in vivo fracture healing and the used models. Firstly, the used models are primarily two dimensional with the fibers relatively sparsely spaced, whereas in vivo tissues are composed of complex three dimensional networks containing densely packed fibers. Furthermore, the used fiber patterns and fiber membranes are fabricated using aligned fibers, whilst early fracture tissues consists of unordered fibers. On top of this, during fracture healing, a dynamic profile of growth factor and cytokine expression can be found. Interactions between these components with both cells and scaffold structure can significantly alter cell behaviour, and were not accounted for in this study. Lastly, in this study, only endothelial cell behaviour was assessed. On the other hand, fracture healing is a multicellular process, in which cell behaviour can be directly altered by the presence of other cell types. Nevertheless, this work has shown the influence of different fiber structures and fibers compositions on cellular migration. As such, it indicates the need to understand cellular behaviour to develop new treatments that can aid in the bone regeneration process. Ultimately, further development of these fiber based models of fracture healing can be used to tackle the socio-economic burden of bone fractures by giving insight in the fracture healing process.

Bibliography

[1] P. Pivonka and C. R. Dunstan, *Role of mathematical modeling in bone fracture healing,* BoneKEy Reports **1** (2012), 10.1038/bonekey.2012.221.

[2] T. A. Einhorn and L. C. Gerstenfeld, *Fracture healing: mechanisms and interventions,* Nature Reviews Rheumatology **11**, 45 (2015).

[3] R. Dimitriou, E. Tsiridis, and P. V. Giannoudis, *Current concepts of molecular aspects of bone healing,* Injury **36**, 1392 (2005).

[4] P. S. Lienemann, M. P. Lutolf, and M. Ehrbar, *Biomimetic hydrogels for controlled biomolecule delivery to augment bone regeneration,* Advanced Drug Delivery Reviews **64**, 1078 (2012).

[5] L. Lamalice, F. Le Boeuf, and J. Huot, *Endothelial Cell Migration During Angiogenesis,* Circulation Research **100**, 782 (2007).

[6] X. Li, Z. Li, L. Wang, G. Ma, F. Meng, R. H. Pritchard, E. L. Gill, Y. Liu, and Y. Y. S. Huang, *Low-Voltage Continuous Electrospinning Patterning,* ACS Applied Materials & Interfaces **8**, 32120 (2016).

[7] S.-i. Harada and G. A. Rodan, *Control of osteoblast function and regulation of bone mass,* Nature **423**, 349 (2003).

[8] L. J. Donaldson, I. P. Reckless, S. Scholes, J. S. Mindell, and N. J. Shelton, *The epidemiology of fractures in England,* Journal of Epidemiology & Community Health **62**, 174 (2008).

[9] M. Panagiotis, *Classification of non-union,* Injury **36**, S30 (2005).

[10] H. S. Leanora Mills, *The relative incidence of fracture non-union in the scottish population (5.17 million): a 5-year epidemiological study,* BMJ Open **3**, e002276 (2013).

[11] J. Leal, D. Prieto-Alhambra, N. K. Arden, C. Cooper, M. K. Javaid, and A. Judge, *Impact of hip fracture on hospital care costs: a population-based study,* Osteoporosis International **27**, 549 (2016).

[12] L. C. Gerstenfeld, D. M. Cullinane, G. L. Barnes, D. T. Graves, and T. A. Einhorn, *Fracture healing as a post-natal developmental process: Molecular, spatial, and temporal aspects of its regulation,* Journal of Cellular Biochemistry **88**, 873 (2003).

[13] A. Atala, R. Lanza, J. Thomson, and R. Nerem, *Principles of Regenerative Medicine* (Elsevier, 2008).

[14] C. Lu, R. Marcucio, and T. Miclau, *Assessing angiogenesis during fracture healing,* Iowa Orthop J **26**, 17 (2006).

[15] P. V. Giannoudis, T. A. Einhorn, and D. Marsh, *Fracture healing: The diamond concept,* Injury **38**, S3 (2007).

[16] R. Marsell and T. A. Einhorn, *The biology of fracture healing,* Injury **42**, 551 (2011).

[17] S. Chen, Y. Guo, R. Liu, S. Wu, J. Fang, B. Huang, Z. Li, Z. Chen, and Z. Chen, *Tuning surface properties of bone biomaterials to manipulate osteoblastic cell adhesion and the signaling pathways for the enhancement of early osseointegration,* Colloids and Surfaces B: Biointerfaces **164**, 58 (2018).

[18] S. Bose, M. Roy, and A. Bandyopadhyay, *Recent advances in bone tissue engineering scaffolds,* Trends in Biotechnology **30**, 546 (2012).

[19] Q. L. Loh and C. Choong, *Three-Dimensional Scaffolds for Tissue Engineering Applications: Role of Porosity and Pore Size,* Tissue Engineering Part B: Reviews **19**, 485 (2013).

[20] V. Karageorgiou and D. Kaplan, *Porosity of 3d biomaterial scaffolds and osteogenesis,* Biomaterials **26**, 5474 (2005).

[21] X. Wang, T. E. Friis, P. P. Masci, R. W. Crawford, W. Liao, and Y. Xiao, *Alteration of blood clot structures by interleukin-1 beta in association with bone defects healing,* Scientific Reports **6** (2016), 10.1038/srep35645.

[22] K. Schmidt-Bleek, H. Schell, N. Schulz, P. Hoff, C. Perka, F. Buttgereit, H.-D. Volk, J. Lienau, and G. N. Duda, *Inflammatory phase of bone healing initiates the regenerative healing cascade,* Cell and Tissue Research **347**, 567 (2012).

[23] F. Loi, L. A. Córdova, J. Pajarinen, T.-h. Lin, Z. Yao, and S. B. Goodman, *Inflammation, fracture and bone repair,* Bone **86**, 119 (2016).

[24] D. Marsh, *Concepts of fracture union, delayed union, and nonunion,* Clin. Orthop. Relat. Res. , S22 (1998).

[25] M. Steiner, L. Claes, A. Ignatius, U. Simon, and T. Wehner, *Numerical Simulation of Callus Healing for Optimization of Fracture Fixation Stiffness,* PLoS ONE **9**, e101370 (2014).

[26] E. Ozcivici, Y. K. Luu, B. Adler, Y.-X. Qin, J. Rubin, S. Judex, and C. T. Rubin, *Mechanical signals as anabolic agents in bone,* Nature Reviews Rheumatology **6**, 50 (2010).

[27] M. Vicente-Manzanares, C. K. Choi, and A. R. Horwitz, *Integrins in cell migration - the actin connection,* Journal of Cell Science **122**, 199 (2009).

[28] N. Jusoh, S. Oh, S. Kim, J. Kim, and N. L. Jeon, *Microfluidic vascularized bone tissue model with hydroxyapatite-incorporated extracellular matrix,* Lab on a Chip **15**, 3984 (2015).

[29] P. Friedl and D. Gilmour, *Collective cell migration in morphogenesis, regeneration and cancer,* Nature Reviews Molecular Cell Biology **10**, 445 (2009).

[30] T. Panetti, D. F. Hannah, C. Avraamides, J. P. Gaughan, C. Marcinkiewicz, A. Huttenlocher, and D. F. Mosher, *Extracellular matrix molecules regulate endothelial cell migration stimulated by lysophosphatidic acid: ECM regulates LPA-stimulated migration,* Journal of Thrombosis and Haemostasis **2**, 1645 (2004).

[31] B. N. Mason, A. Starchenko, R. M. Williams, L. J. Bonassar, and C. A. Reinhart-King, *Tuning three-dimensional collagen matrix stiffness independently of collagen concentration modulates endothelial cell behavior,* Acta Biomaterialia **9**, 4635 (2013).

[32] J. Solon, I. Levental, K. Sengupta, P. C. Georges, and P. A. Janmey, *Fibroblast Adaptation and Stiffness Matching to Soft Elastic Substrates,* Biophysical Journal **93**, 4453 (2007).

[33] Sukhyun, S., M. Kim, and J. Shin, *Upstream mechanotaxis behavior of endothelial cells,* (IEEE, 2009) pp. 2106–2110.

[34] S. Chang, W.-h. Guo, Y. Kim, and Y.-l. Wang, *Guidance of Cell Migration by Substrate Dimension,* Biophysical Journal **104**, 313 (2013).

[35] J. Condeelis and J. E. Segall, *Intravital imaging of cell movement in tumours,* Nature Reviews Cancer **3**, 921 (2003).

[36] A. M. Sitarski, H. Fairfield, C. Falank, and M. R. Reagan, *3d Tissue Engineered in Vitro Models of Cancer in Bone,* ACS Biomaterials Science & Engineering **4**, 324 (2018).

[37] B. Robb and B. Lennox, *The electrospinning process, conditions and control,* in *Electrospinning for Tissue Regeneration* (Elsevier, 2011) pp. 51–66.

[38] M. C. Echave, L. S. Burgo, J. L. Pedraz, and G. Orive, *Gelatin as Biomaterial for Tissue Engineering,* Current Pharmaceutical Design **23** (2017), 10.2174/0929867324666170511123101.

[39] M. P. Francis, Y. M. Moghaddam-White, P. C. Sachs, M. J. Beckman, S. M. Chen, G. L. Bowlin, L. W. Elmore, and S. E. Holt, *Modeling early stage bone regeneration with biomimetic electrospun fibrinogen nanofibers and adipose-derived mesenchymal stem cells,* Electrospinning **1** (2016), 10.1515/esp-2016-0002.

[40] H. M. Estabridis, A. Jana, A. Nain, and D. J. Odde, *Cell Migration in 1d and 2d Nanofiber Microenvironments,* Annals of Biomedical Engineering **46**, 392 (2018).

[41] M. Ahmed, T. Ramos, P. Wieringa, C. v. Blitterswijk, J. d. Boer, and L. Moroni, *Geometric constraints of endothelial cell migration on electrospun fibres,* Scientific Reports **8** (2018), 10.1038/s41598-018-24667-7.

[42] N. Kramer, A. Walzl, C. Unger, M. Rosner, G. Krupitza, M. Hengstschläger, and H. Dolznig, *In vitro cell migration and invasion assays,* Mutation Research/Reviews in Mutation Research **752**, 10 (2013).

[43] N. Xue, X. Li, C. Bertulli, Z. Li, A. Patharagulpong, A. Sadok, and Y. Y. S. Huang, *Rapid Patterning of 1-D Collagenous Topography as an ECM Protein Fibril Platform for Image Cytometry,* PLoS ONE **9**, e93590 (2014).

[44] S. L. Rowe, S. Lee, and J. P. Stegemann, *Influence of thrombin concentration on the mechanical and morphological properties of cell-seeded fibrin hydrogels,* Acta Biomaterialia **3**, 59 (2007).

[45] J. S. Jeon, S. Bersini, M. Gilardi, G. Dubini, J. L. Charest, M. Moretti, and R. D. Kamm, *Human 3d vascularized organotypic microfluidic assays to study breast cancer cell extravasation,* Proceedings of the National Academy of Sciences **112**, 214 (2015).

[46] G. E. Wnek, M. E. Carr, D. G. Simpson, and G. L. Bowlin, *Electrospinning of Nanofiber Fibrinogen Structures,* Nano Letters **3**, 213 (2003).

[47] R. Litvinov, D. Faizullin, Y. Zuev, and J. Weisel, *The a-Helix to b-Sheet Transition in Stretched and Compressed Hydrated Fibrin Clots,* Biophysical Journal **103**, 1020 (2012).

[48] J. S. Nowick, *Exploring β-Sheet Structure and Interactions with Chemical Model Systems,* Accounts of Chemical Research **41**, 1319 (2008).

[49] D. I. Zeugolis, S. T. Khew, E. S. Yew, A. K. Ekaputra, Y. W. Tong, L.-Y. L. Yung, D. W. Hutmacher, C. Sheppard, and M. Raghunath, *Electro-spinning of pure collagen nano-fibres – Just an expensive way to make gelatin?* Biomaterials **29**, 2293 (2008).

[50] M. J. Mirzaei-Parsa, A. Ghanizadeh, M. T. Ebadi, and R. Faridi-Majidi, *An alternative solvent for electrospinning of fibrinogen nanofibers,* Bio-Medical Materials and Engineering **29**, 279 (2018).

[51] B. S. Jha, C. E. Ayres, J. R. Bowman, T. A. Telemeco, S. A. Sell, G. L. Bowlin, and D. G. Simpson, *Electrospun Collagen: A Tissue Engineering Scaffold with Unique Functional Properties in a Wide Variety of Applications,* Journal of Nanomaterials **2011**, 1 (2011).

[52] M. Lunova, V. Zablotskii, N. M. Dempsey, T. Devillers, M. Jirsa, E. Syková, . Kubinová, O. Lunov, and A. Dejneka, *Modulation of collective cell behaviour by geometrical constraints,* Integrative Biology **8**, 1099 (2016).

[53] Q. Zhang, H. Dong, Y. Li, Y. Zhu, L. Zeng, H. Gao, B. Yuan, X. Chen, and C. Mao, *Microgrooved Polymer Substrates Promote Collective Cell Migration To Accelerate Fracture Healing in an in Vitro Model,* ACS Applied Materials & Interfaces **7**, 23336 (2015).

[54] I. A. Relou, C. A. Damen, D. W. van der Schaft, G. Groenewegen, and A. W. Griffioen, *Effect of culture conditions on endothelial cell growth and responsiveness,* Tissue and Cell **30**, 525 (1998).

[55] X. Wang, T. Friis, V. Glatt, R. Crawford, and Y. Xiao, *Structural properties of fracture haematoma: current status and future clinical implications: Structural properties of fracture haematoma,* Journal of Tissue Engineering and Regenerative Medicine **11**, 2864 (2017).

[56] Y. Yang, N. Jamilpour, B. Yao, Z. S. Dean, R. Riahi, and P. K. Wong, *Probing Leader Cells in Endothelial Collective Migration by Plasma Lithography Geometric Confinement,* Scientific Reports **6** (2016), 10.1038/srep22707.

[57] S. Javaherian, K. A. O'Donnell, and A. P. McGuigan, *A Fast and Accessible Methodology for Micro-Patterning Cells on Standard Culture Substrates Using Parafilm™ Inserts,* PLoS ONE **6**, e20909 (2011).

[58] Z. Chen, J. Yang, B. Wu, and B. Tawil, *A Novel Three-Dimensional Wound Healing Model,* Journal of Developmental Biology **2**, 198 (2014).

[59] P. Sharma, C. Ng, A. Jana, A. Padhi, P. Szymanski, J. S. H. Lee, B. Behkam, and A. S. Nain, *Aligned fibers direct collective cell migration to engineer closing and nonclosing wound gaps,* Molecular Biology of the Cell **28**, 2579 (2017).

[60] M. Matsuda, M. Sawa, H. F. Edelhauser, S. P. Bartels, A. H. Neufeld, and K. R. Kenyon, *Cellular migration and morphology in corneal endothelial wound repair,* Invest. Ophthalmol. Vis. Sci. **26**, 443 (1985).

[61] X. Feng, M. G. Tonnesen, S. A. Mousa, and R. A. F. Clark, *Fibrin and Collagen Differentially but Synergistically Regulate Sprout Angiogenesis of Human Dermal Microvascular Endothelial Cells in 3-Dimensional Matrix,* International Journal of Cell Biology **2013**, 1 (2013).

[62] J. Shepherd, D. Bax, S. Best, and R. Cameron, *Collagen-Fibrinogen Lyophilised Scaffolds for Soft Tissue Regeneration,* Materials **10**, 568 (2017).

[63] S. Baker, J. Sigley, C. C. Helms, J. Stitzel, J. Berry, K. Bonin, and M. Guthold, *The mechanical properties of dry, electrospun fibrinogen fibers,* Materials Science and Engineering: C **32**, 215 (2012).

[64] C. Carlisle, C. Coulais, and M. Guthold, *The mechanical stress–strain properties of single electrospun collagen type I nanofibers,* Acta Biomaterialia **6**, 2997 (2010).

[65] V. Hakim and P. Silberzan, *Collective cell migration: a physics perspective,* Reports on Progress in Physics **80**, 076601 (2017).

[66] S. Eom, S. M. Park, S. J. Han, J. W. Kim, and D. S. Kim, *One-step fabrication of a tunable nanofibrous well insert via electrolyte-assisted electrospinning,* RSC Advances **7**, 38300 (2017).

[67] V. C.-H. Tseng, C. H. Chew, W.-T. Huang, Y.-K. Wang, K.-S. Chen, S.-Y. Chou, and C.-C. Chen, *An Effective Cell Coculture Platform Based on the Electrospun Microtube Array Membrane for Nerve Regeneration,* Cells Tissues Organs **204**, 179 (2017).

[68] K. Wolf, M. te Lindert, M. Krause, S. Alexander, J. te Riet, A. L. Willis, R. M. Hoffman, C. G. Figdor, S. J. Weiss, and P. Friedl, *Physical limits of cell migration: Control by ECM space and nuclear deformation and tuning by proteolysis and traction force,* The Journal of Cell Biology **201**, 1069 (2013).

[69] K. Duval, H. Grover, L.-H. Han, Y. Mou, A. F. Pegoraro, J. Fredberg, and Z. Chen, *Modeling Physiological Events in 2d vs. 3d Cell Culture,* Physiology **32**, 266 (2017).

[70] B. M. Whited and M. N. Rylander, *The influence of electrospun scaffold topography on endothelial cell morphology, alignment, and adhesion in response to fluid flow: Electrospun Topography Effects EC Adhesion,* Biotechnology and Bioengineering **111**, 184 (2014).